

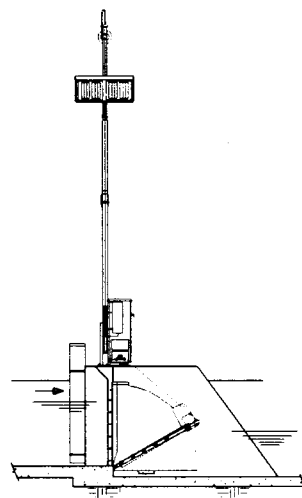
# Flow Measurement Using An Overshot Gate

By: B.T. Wahlin and J. A. Replogle

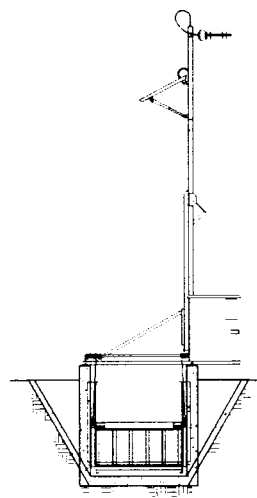
This research was supported by the

UNITED STATES  
DEPARTMENT OF THE INTERIOR  
BUREAU OF RECLAMATION

under **Cooperative Agreement No. 1425-2-FC-81-19060** entitled  
Water Conservation Innovative Technology Research  
For Agriculture and Urban Irrigation Water



SECTION VIEW



DOWNSTREAM VIEW

Public reporting burden for this collection of information is estimated to average 1 hour per response, including the time for reviewing instructions, searching existing data sources, gathering and maintaining the data needed, and completing and reviewing the collection of information. Send comments regarding this burden estimate or any other aspect of this collection of information, including suggestions for reducing the burden to Washington Headquarters Services, Directorate for Information Operations and Reports, 1215 Jefferson Davis Highway, Suit 1204, Arlington VA 22202-4302, and to the Office of Management and Budget, Paperwork Reduction Project (0704-0188), Washington DC 20503.

1. AGENCY USE ONLY (Leave Blank)	2. REPORT DATE August 1994	3. REPORT TYPE AND DATES COVERED
----------------------------------	-------------------------------	----------------------------------

4. TITLE AND SUBTITLE Flow Measurement Using an Overshot Gate	5. FUNDING NUMBERS
--	--------------------

6. AUTHOR(S) B. T. Wahlin and J. A. Replogle	
---	--

7. PERFORMING ORGANIZATION NAME(S) AND ADDRESS(ES) UMA Engineering, Inc.	8. PERFORMING ORGANIZATION REPORT NUMBER
---	--

9. SPONSORING/MONITORING AGENCY NAME(S) AND ADDRESS(ES) United States Department of the Interior Bureau of Reclamation PO Box 25007, D-8560 Denver CO 80225-0007	10. SPONSORING/MONITORING AGENCY REPORT NUMBER
--	--

11. SUPPLEMENTARY NOTES Research performed under Cooperative Agreement No. 1425-2-FC-81-19060 entitled Water Conservation Innovative Technology Research for Agriculture and Urban Irrigation Water.
---

12a. DISTRIBUTION/AVAILABILITY STATEMENT	12b. DISTRIBUTION CODE
--	------------------------

13. ABSTRACT (Maximum 200 words) Overshot gates, or leaf gates as they are sometimes called, are becoming increasingly popular for controlling water levels in open canals. This popularity is partly due to the ability of the gates to handle flow surges with limited depth changes and the ease with which operators can understand the hydraulic behavior of the gates. While water level control is useful, operators also need to know the flow rate at each gate to better operate the system. While existing theories provide some background for the overshot gate hydraulics, this study focused on information specific to inclined weirs. Equations derived from this study can be used to accurately determine flow rate in the field of a properly ventilated free-flow leaf gate to within 6.4 percent. Additional equations are provided to predict the discharge of a submerged overshot gate with an accuracy of roughly 10 percent.
--

14. SUBJECT TERMS water measurement/canals/gates/laboratory tests/field tests/accuracy/free flow/submerged flow/discharge coefficients	15. NUMBER OF PAGES 45
	16. PRICE CODE

17. SECURITY CLASSIFICATION OF REPORT	18. SECURITY CLASSIFICATION OF THIS PAGE	19. SECURITY CLASSIFICATION OF ABSTRACT	20. LIMITATION OF ABSTRACT
---------------------------------------	--	---	----------------------------

**Abstract:**

Recently, overshot gates, or leaf gates as they are sometimes called, are becoming increasingly popular for controlling water levels in open channels. This popularity is partly due to the ability of the gates to handle flow surges with limited depth changes and the ease with which operators can understand the hydraulic behavior of the gates. With an overshot gate a 10-cm drop in gate height corresponds closely to a 10-cm drop in upstream water level. While water level control is useful, operators also need to know the flow rate at each gate to better operate the system. At high gate angles, the overshot gate appears to resemble a sharp-crested weir while at low gate angles it looks as if it might behave more like a free overfall.

While existing theories provide some background for the overshot gate hydraulics, this study focused on information specific to inclined weirs. The theoretical evaluation was tested against hydraulic lab modeling and field investigations. Equations derived can be used to accurately determine the flow rate in the field of a properly ventilated free-flow leaf gate to within approximately 6.4% with a standard deviation of around 3.2%. These equations are valid for values of  $h_1/p$  less than 1.0 and for gate angles between 16.2° and 63.4°. Additional equations can be used to predict the discharge of a submerged overshot gate with an accuracy of roughly 10%.

**List of Key Words:**

water measurement/ canals/ gates/ laboratory tests/ field tests/ accuracy/ free flow/ submerged flow/ discharge coefficients



# Flow Measurement Using An Overshot Gate

By: B. T. Wahlin and J. A. Replogle

## TECHNICAL SUMMARY

Recently, overshot gates, or leaf gates as they are sometimes called, are becoming increasingly popular for controlling water levels in open channels. This popularity is partly due to the ability of the gates to handle flow surges with limited depth changes and the ease with which operators can understand the hydraulic behavior of the gates.

The main purpose of most control gates is to maintain a constant water depth upstream so that orifice-based offtakes, usually located just upstream of the gates, will deliver water at a near-constant rate regardless of the flow rate in the main canal. The control gates themselves can either be orifice-based gates, such as sluice or radial gates, or weir-type gates. Generally, weirs are able to control water surfaces more closely than orifice gates because the water level upstream varies with the three-halves power of the head over the weir. Overshot gates are also more intuitive to operate because a 10-cm drop in gate height corresponds closely to a 10-cm drop in upstream water level.

While water level control is useful, operators also need to know the flow rate at each gate to better operate the system. At high gate angles, the overshot gate appears to resemble a sharp-crested weir while at low gate angles it looks as if it might behave more like a free overfall.

Kindsvater and Carter (1959) presented a form of the discharge equation for either a fully or partially contracted sharp-crested vertical weir. They considered the effect of the viscous and surface tension forces and introduced an effective discharge coefficient,  $C_e$ . The viscous and surface tension forces were accounted for by modifying the width of the weir and the head approaching the weir. The final form of Kindsvater and Carter's discharge equation is as follows:

$$Q = C_e \frac{2}{3} \sqrt{2g} b_e h_e^{1.5} \quad [A]$$

where  $C_e$  = effective discharge coefficient;  
 $g$  = gravitational acceleration ( $9.81 \text{ m/s}^2$ );  
 $b_e$  = effective width of the weir; and  
 $h_e$  = effective head on the weir.

The effective width of the weir is expressed in terms of an empirical constant,  $K_b$ , that depends on the ratio  $b_c/B_1$  (where  $b_c$  = width of the overshot gate and  $B_1$  = width of approach channel) as follows:

$$b_e = b_c + K_b \quad [B]$$

In a similar way, the effective head can be expressed in terms of another empirical constant,  $K_h$ , as follows:

$$h_e = h_1 + K_h \quad [C]$$

Kindsvater and Carter (1959) showed that the effective discharge coefficient varies linearly with  $b_c/B_1$  and  $h_1/p$  only (where  $p$  = height of weir from channel bottom to crest). The value of  $C_e$  is assumed to be of the form:

$$C_e = m \frac{h_1}{p} + b \quad [D]$$

where  $m$  and  $b$  = empirical constants.

The overfall edge of a leaf gate is in an area of no side contraction; therefore, the effective discharge coefficient can be calculated assuming no side contractions of the weir. Thus, Kindsvater and Carter (1959) use  $m = 0.075$  and  $b = 0.602$  to calculate the effective discharge coefficient. Because it was assumed that there was no effects due to side contractions, a value of  $-0.001$  m ( $-0.003$  ft) can be assigned to  $K_b$ . Kindsvater and Carter (1959) also recommend that a constant value of  $0.001$  m ( $0.003$  ft) be assigned to  $K_a$  regardless of the flow rate or gate height.

It was found that Kindsvater and Carter's discharge equation for sharp-crested weirs will also apply to overshot gates if an appropriate value of  $C_e$  is accurately determined with respect to the gate angle. Equation A was used to calculate the discharge over a leaf gate by modifying it with another discharge coefficient as follows:

$$Q = C_a C_e \frac{2}{3} \sqrt{2g} b_e h_e^{1.5} \quad [E]$$

where  $C_a$  = correction factor for angle of the gate; and  
 $C_e$  = effective discharge coefficient for a vertical weir.

An empirical expression for  $C_a$  was determined from laboratory tests. For values of  $h_1/p$  less than 1.0 and for gate angles between  $16.2^\circ$  and  $63.4^\circ$ ,  $C_a$  can be described as follows:

$$C_a = 1.0333 + 0.003848\theta - 0.000045\theta^2 \quad [F]$$

where  $\theta$  = gate angle in degrees.

When the overshot gate is operating under submerged conditions, Kindsvater and Carter's discharge coefficient is further modified as follows:

$$Q = C_{df} C_a C_e \frac{2}{3} \sqrt{2g} b_e h_e^{1.5} \quad [G]$$

where  $C_{df}$  = a drowned flow reduction factor.

Villemonthe (1947) proposed the following form of  $C_{df}$ :

$$C_{df} = A \left[ 1 - \left( \frac{h_2}{h_1} \right)^{1.5} \right]^n \quad [H]$$

where  $h_1$  = upstream measured head;  
 $h_2$  = downstream measured head; and  
 $A$  and  $n$  = empirical coefficients.

The following empirical equations can be used to describe  $A$  and  $n$  if the value of  $h_1/p$  is less than 1.0, the gate angle is between  $16.2^\circ$  and  $63.4^\circ$ , and the submergence ratio is less than 0.90:

$$\begin{aligned} A &= -0.0013\theta + 1.0663 && \text{for } \theta < 60^\circ \\ A &= 1.0 && \text{for } \theta > 60^\circ \end{aligned} \quad [I]$$

$$n = 0.1525 + 0.006077\theta - 0.000045\theta^2 \quad [J]$$

where  $\theta$  = gate angle in degrees.

From laboratory and field studies, it is believed that Equations E and F will provide field measurement accuracy of 6.4% for typical field installations. We have insufficient field verification to judge the accuracy of submerged overshot gates. At this time, the accuracy of the submerged gates is roughly estimated to be 10%. This accuracy estimation does not include errors associated with head measurement. Errors in head measurement will be much greater under submerged conditions than under free-flow conditions, particularly due to the difficulty of making downstream head measurements.

### TECHNICAL EXAMPLE

As an example, consider a leaf gate in the field that is 2 m wide, 3 m long, and is mounted on a 7.5 cm square channel. To determine the discharge, the head on the gate,  $h_1$ , and the height of the crest above the channel bottom,  $p$ , must be determined. Because the value of  $C_a$  and  $C_e$  change very slowly with gate angle and  $h_1/p$ , it is more important to determine  $h_1$  accurately than  $p$ . To continue the example, assume that  $h_1 = 1.00$  m and  $p = 2.00$  m. These two values yield an  $h_1/p$  of 0.50. The gate angle can then be calculated using the following equation:

$$\theta = \arcsin\left(\frac{p-t}{L}\right) \quad [K]$$

where  $\theta$  = gate angle in degrees;

$p$  = height of gate crest above the channel bottom (2.00 m);

$t$  = height of square channel that the overshot gate is mounted on (0.075 m); and

$L$  = length of the overshot gate blade in the direction of flow (3 m).

Using Equation K, the gate angle is found to be equal to 39.9°. Because  $h_1/p$  is less than 1.0 and the gate angle is between 16.2° and 63.4°, Equation F can be used to determine that  $C_a = 1.115$ . Using Equation D, the  $C_e$  can be found to equal 0.640. Finally, Equation E can be used to determine that the discharge is 4,216 l/s. Table A is a sample rating table for this example under free-flow conditions for various values of  $h_1$  and  $p$ .

Next, consider the same gate operating under submerged conditions. Assume that  $h_1$  and  $p$  are the same for the free-flow case and that the downstream head,  $h_2$ , is 0.30 m. Using these values, the submergence ratio ( $h_2/h_1$ ) is 0.30. Because  $h_1/p$  is less than 1.0, the submergence ratio is less than 0.90, and the gate angle is between 16.2° and 63.4°, Equations I and J can be used to estimate that  $A = 1.014$  and  $n = 0.323$ . Using Equation H, the drowned flow reduction factor can be found equal to 0.957, and the new discharge would therefore be 4,036 l/s.

		$p$ (m)			
		1.0	1.5	2.0	2.5
$h_1$ (m)	0.25	501	505	506	505
	0.50	1,456	1,452	1,449	1,444
	0.75	2,751	2,718	2,700	2,663
	1.00	4,354	4,264	4,216	4,147
	1.25		6,072	5,977	5,863
	1.50		8,130	7,969	7,796

Table A: Discharge in l/s of example free-flow overshot gate for a various values of  $h_1$  and  $p$ .



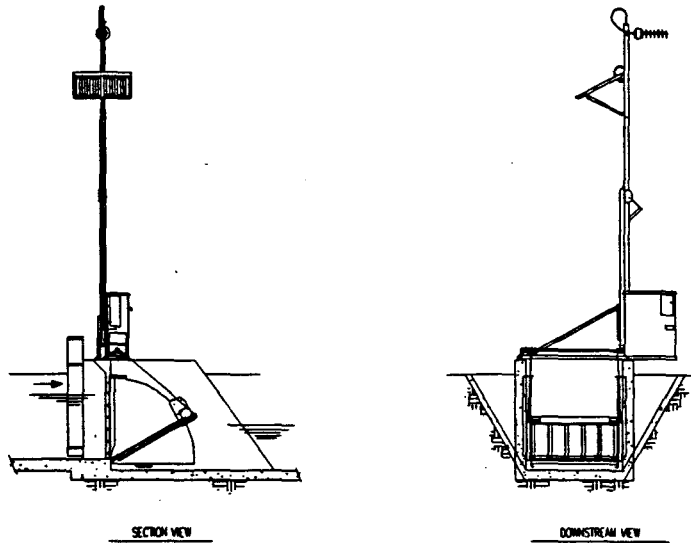
# Flow Measurement Using An Overshot Gate

By: B.T. Wahlin and J. A. Replogle

This research was supported by the

UNITED STATES  
DEPARTMENT OF THE INTERIOR  
BUREAU OF RECLAMATION

under Cooperative Agreement No. 1425-2-FC-81-19060 entitled  
Water Conservation Innovative Technology Research  
For Agriculture and Urban Irrigation Water



Submitted by:

**Uma** Engineering, Inc.

August 1994



## **ACKNOWLEDGEMENTS**

This research was undertaken by a joint effort of UMA Engineering and Agricultural Reserach Service (ARS), U.S. Water Conservation Lab in Phoenix. B.T. Wahlin and J.A. Replogle completed all laboatory research and were assisted in the field verification by David Bradshaw of UMA Engineering. The efforts were coordinated and reviewed by Albert J. Clemmens, Research Leader (ARS) and John H. Korinetz, Project Manager (UMA).

The Contracting Officer's Technical Representativie's were Danny L. King and Philip H. Burgi. In addition to finiancial support the USBR also provided technical review, Brent Mefford participated in technical review of the research.

Armtec Water Control Products provided a manual overshot gate for the laboratory research.

The Imperial Irrigation District (IID) extended their cooperation to make the field testing possible. Dave Merkley, John Van Bebber and the Holtville divison staff, provided liason with the irrigators and provided district cooperation to the research.

## **NOTATIONS**

**"This manuscript is submitted for publication with the understanding that the United States Government is authorized to reproduce and distribute reprints for governmental purposes."**

**"The views and conclusions contained in this document are those of the authors and should not be interpreted as necessarily representing the offical policies, either express or implied, of the U.S. Government."**

**The United States Government does not endorse products or manufacturers. Trade or manufacturer's names appear herein only because they are considered essential to the object of this document.**



## CONTENTS

	Page
Introduction	1
Background Theory	2
Laboratory Tests	8
Results	11
Discussion of Results	18
Conclusions	24

## Appendices

Appendix I. - References

Appendix II. - Glossary

Appendix III. - Data for Free-overfall Armtec overshoot gate

Appendix IV. - Data for Free-overfall Armtec overshoot gate w/side contractions

Appendix V. - Data for Submerged Armtec overshoot gate

Appendix VI. - Data for Submerged Armtec overshoot gate w/side contractions

Appendix VII. - Data for Free-overfall USWCL overshoot gate

Appendix VIII. - Data for Bazin's experiments on inclined weirs

Appendix IX. - Data for USBR's experiments on inclined weirs

Appendix X. - Data for Field experiments on free-overfall inclined weirs



## INTRODUCTION

Recently, overshot gates, or dropleaf gates as they are sometimes called, have become increasingly popular for controlling water levels in open channels. This popularity is partly due to the ability of the gates to handle flow surges with limited depth changes and the ease with which operators can understand the hydraulic behavior of the gates.

The overshot gate was introduced by UMA Engineering for controlling irrigation water in such places as the St. Mary River Irrigation District in Lethbridge, Alberta, and South San Joaquin Irrigation District (SSJID) and the Imperial Irrigation District (IID) in southern California. The Salt River Project (SRP) in Phoenix, Arizona, also uses them in flood control spillways. The basic layout of an overshot gate is simple. It consists of a rectangular panel that is hinged to the bottom of the canal. Usually, two cables connect the top of the panel to a hoisting mechanism that can then be used to raise and lower the gate to the desired height to control the upstream depth for various flow rates (Figure 1).

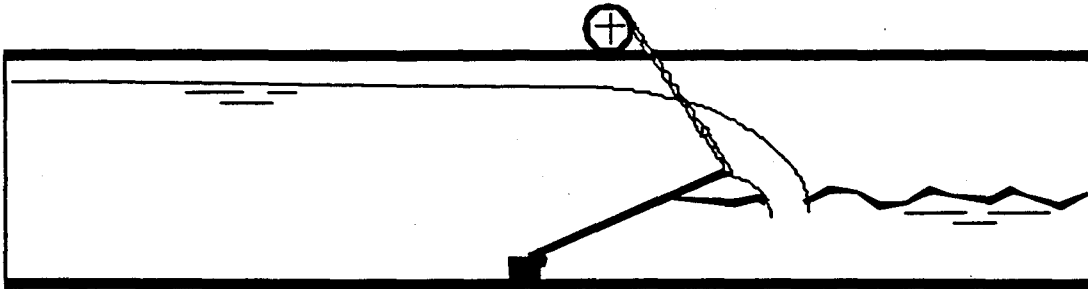


Figure 1: General schematic of an overshot gate.

The main purpose of most control gates is to maintain a constant water depth upstream so that orifice-based offtakes, usually located just upstream of the gates, will deliver water at a near-constant rate regardless of the flow rate in the main canal. The control gates themselves can either be orifice-based gates, such as sluice or radial gates, or weir-type gates. Generally, weirs are able to control water surfaces more closely than orifice gates because the water level upstream varies with the three-halves power of the head over the weir. This means that changes in flow rates will not create much change in the upstream water surface elevation. Upstream water levels for an orifice gate, on the other hand, vary with the one-half power of the head approaching the gate. Thus, for a given setting, orifice-based gates usually produce large fluctuations in water surface elevations from changes in flow rates compared to weirs. However, the height of simple weir structures is not readily adjustable and is usually changed incrementally with stop log checks. Orifice gates are easily adjusted to any gate opening the operator desires. They are better suited to good downstream flow rate control rather than upstream water level control because accurate control of the water level requires more hydraulic understanding and more accurate adjustments on the part of the operator. Overshot gates are more intuitive to operate because a 10-cm drop in gate height corresponds closely to a 10-cm drop in upstream water level.

While water level control is useful, operators also need to know the flow at each gate to better operate the system. At high gate angles, the overshot gate appears to resemble a sharp-crested weir while at low gate angles it looks as if it might behave more like a free overfall. It seemed likely that the discharge could be determined by using a modified version of a sharp-crested weir discharge formula. Thus, laboratory studies were performed in an attempt to evaluate the hydraulic characteristics of the overshot gate. Because the overshot gate can be operated in the field under both free-flow and submerged conditions, tests were performed for both circumstances.

## BACKGROUND THEORY

### Free-Flow Weirs

The head on a sharp-crested weir increases with discharge. An equation predicting this behavior was derived by assuming that the sharp-crested weir behaves like half of an orifice with a free surface in place of the upper half and by using the following simplifying assumptions (Bos, 1989):

1. there is no contraction of the water surface above the crest;
2. the streamlines over the crest are horizontal;
3. the approach velocity head is negligible;
4. the viscous and surface tension forces are negligible; and
5. the friction losses between the head measurement location and the crest are negligible.

The velocity of an arbitrary point at the control section of the weir can be calculated using Torricelli's equation (Bos, 1989):

$$v = \sqrt{2g(h_1 - y)} \quad [1]$$

where  $v$  = velocity of an arbitrary point in the control section;  
 $g$  = gravitational acceleration;  
 $h_1$  = measured head approaching the weir; and  
 $y$  = height of arbitrary point above the weir crest (see Figure 2).

The discharge over the weir can then be calculated by integrating Torricelli's velocity equation from  $y = 0$  to  $y = h_1$  as follows:

$$Q = \int_0^{h_1} v b_c dy = \frac{2}{3} C_c \sqrt{2g} b_c h_1^{1.5} \quad [2]$$

where  $Q$  = discharge over the weir;  
 $b_c$  = width of the control section; and  
 $C_c$  = coefficient of contraction.

The five assumptions stated above do not accurately describe what really occurs as water flows over the weir. The contraction coefficient,  $C_c$ , is used to correct for the contraction of the water surface as it flows over the weir crest (assumption 1). Additional correction factors can also be utilized to account for the inadequacies of the remaining four assumptions. To simplify the discharge equation, another discharge coefficient,  $C_d$ , that accounts for all five of the assumptions is usually utilized as follows:

$$Q = C_d \frac{2}{3} \sqrt{2g} b_c h_1^{1.5} \quad [3]$$

where  $C_d$  = discharge coefficient to correct for all of the assumptions.

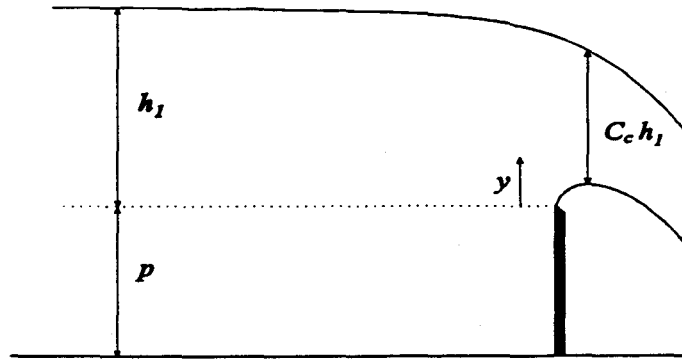


Figure 2: Definition of terms for a sharp-crested weir.

Horton (1907) outlines many specifications that must be followed in order to ensure reasonable accuracy in discharge measurements for sharp-crested weirs using Equation 3. These specifications can be summarized as follows:

1. the upstream crest edge should be smooth and sharp;
2. the nappe should only touch the upstream crest corner;
3. the nappe should be perfectly aerated;
4. the upstream face of the weir should be vertical;
5. the crest should be level from end to end;
6. the approach velocity distribution should be uniform; and
7. the head measurements should show the true water surface elevation above the crest level.

Kindsvater and Carter (1959) presented a slightly different form of the discharge equation for either a fully or partially contracted sharp-crested weir. They removed the effect of the viscous and surface tension forces from  $C_d$  and introduced a new discharge coefficient,  $C_e$ . The viscous and surface tension forces were accounted for by modifying the width of the weir and the head approaching the weir. The final form of Kindsvater and Carter's discharge equation is as follows:

$$Q = C_e \frac{2}{3} \sqrt{2g} b_e h_e^{1.5} \quad [4]$$

where  $C_e$  = effective discharge coefficient;  
 $b_e$  = effective width of the weir; and  
 $h_e$  = effective head on the weir.

The effective width of the weir is expressed in terms of an empirical constant,  $K_b$ , that depends on the ratio  $b_e/B_1$  (where  $B_1$  = width of approach channel) as follows:

$$b_e = b_c + K_b \quad [5]$$

In a similar way, the effective head can be expressed in terms of another empirical constant,  $K_h$ , as follows:

$$h_e = h_1 + K_h \quad [6]$$

Both  $K_b$  and  $K_h$  are used to account for viscous and surface tension forces. The value for  $K_b$  can be obtained from Figure 3, and Kindsvater and Carter (1959) recommend that a constant value of 0.001 m (0.003 ft) be assigned to  $K_h$  regardless of the flow rate or gate height.

At low heads, when viscous and surface tension forces are relatively high, the terms  $K_b$  and  $K_h$  will have a pronounced effect on the discharge equation. Conversely,  $K_b$  and  $K_h$  will have little effect on the flow rate when the heads are high and the viscous and surface tension forces are relatively low. Kindsvater and Carter (1959) showed that the effective discharge coefficient varies linearly with  $b_c/B_1$  and  $h_1/p$  only (where  $p$  = height of weir from channel bottom to crest). The value of  $C_e$  is assumed to be of the form:

$$C_e = m \frac{h_1}{p} + b \quad [7]$$

where  $m$  and  $b$  = empirical constants given in Table 1.

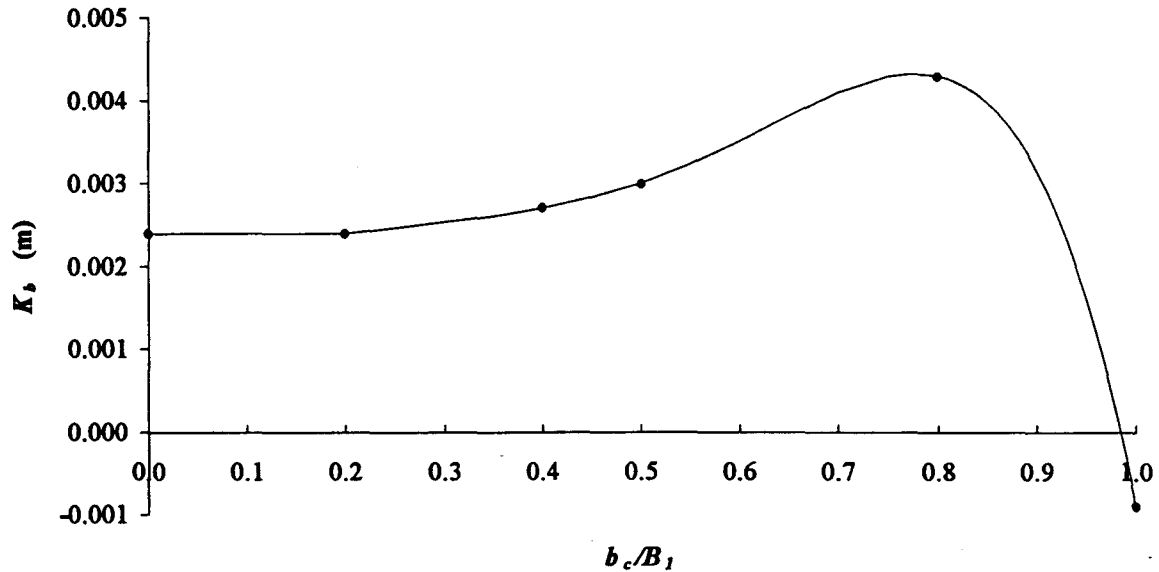


Figure 3: Values of  $K_b$  versus  $b_c/B_1$  (adapted from Kindsvater and Carter, 1959)

$b_c/B_1$	$m$	$b$	$b_c/B_1$	$m$	$b$
1.0	0.075	0.602	0.5	0.011	0.592
0.9	0.064	0.599	0.4	0.0058	0.591
0.8	0.045	0.597	0.3	0.0020	0.590
0.7	0.030	0.595	0.2	-0.0018	0.589
0.6	0.018	0.593	0.1	-0.0021	0.588
			0	-0.0023	0.587

Table 1: Values of  $m$  and  $b$  as a function of  $b_c/B_1$  (from Bos, 1989).

It is expected that Kindsvater and Carter's discharge equation for sharp-crested weirs will also apply to overshoot gates if an appropriate value of  $C_e$  can be accurately determined with respect to the gate angle. It was assumed that Equation 4 could be used to calculate the discharge over a leaf gate if it were modified by another discharge coefficient as follows:

$$Q = C_a C_e \frac{2}{3} \sqrt{2g} b_s h_s^{1.5}$$

[8]

where  $C_a$  = correction factor for angle of the gate; and  
 $C_e$  = effective discharge coefficient for a vertical weir.

The general trend of  $C_a$  can be determined as a function of the gate angle by considering the data presented by the US Bureau of Reclamation (USBR) in its study on crests for overfall dams (1948). Some of the USBR's research was done on inclined sharp-crested weirs, which are similar to overshoot gates. Using the tables presented by the USBR, the shapes of the upper and lower nappes were determined for a full-width weir at various angles of inclination with the following dimensions: width of crest = 1.2 m (4.0 ft); discharge = 387 l/s (13.7 cfs); and measured head = 0.30 m (1.0 ft). The weir height,  $p$ , for the vertical weir was set equal to 0.61 m (2.0 ft) so that the value of  $h_1/p$  equaled 0.5. As the weir angle of inclination was decreased, the face of the weir was increased so that  $h_1/p$  and  $Q$  would remain constant. Upper and lower nappe profiles for inclined weir angles of 90.00°, 71.57°, 56.31°, 45.00°, 26.57°, and 14.04° were determined from the USBR's tables (Figure 4).

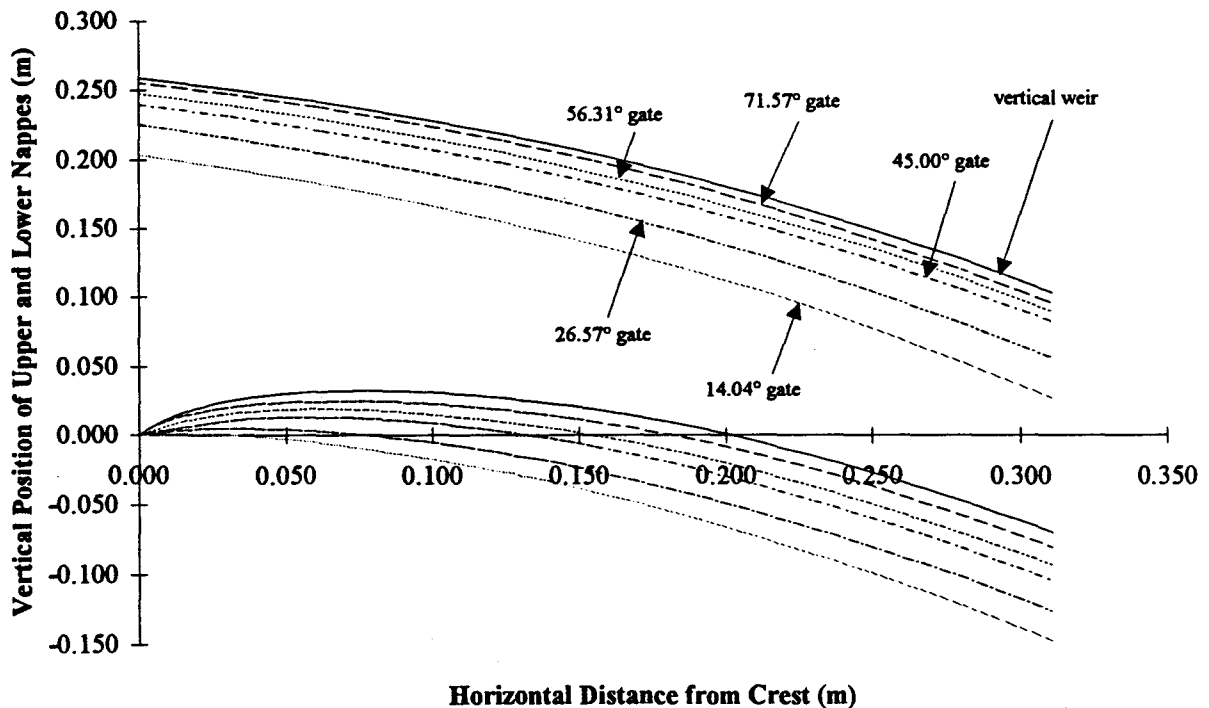


Figure 4: USBR upper and lower nappe profiles for various inclined weir angles.  
 $[Q = 387 \text{ l/s (13.7 cfs)}; h_1 = 0.30 \text{ m (1.0 ft)}]$

From this analysis, the thickness of the *vena contracta* can also be determined for each of the angles of inclination considered (Table 2). As the angle is decreased from the vertical position, the thickness of the *vena contracta* begins to increase. This trend continues until a maximum thickness is reached at a weir angle of about 45°. After this point, the thickness of the *vena contracta* begins to decrease. The contraction coefficient,  $C_c$ , given in Equation 2 is the ratio between the thickness of the *vena contracta* and the approaching head on the weir and can be expressed as follows:

$$C_c = \frac{d}{h_1}$$

[9]

where  $d$  = thickness of the *vena contracta*.

Because both the head and the thickness of the *vena contracta* are known, the contraction coefficient can be calculated for each angle of inclination (Table 2). The *vena contracta* for 0° angle of inclination (or free overfall) was assumed to be equal to the brink depth. The brink depth of a free overfall is approximately  $0.712y_c$ , where  $y_c$  is the critical depth (Rouse, 1936). The contraction coefficient,  $C_c$ , varies with angle of inclination in the same manner as the thickness of the *vena contracta* (Figure 5). Because the effective discharge coefficient,  $C_e$ , used in Equation 8 is assumed to be that of a vertical weir,  $C_e$  must be used to account for the changes in the contraction coefficient as the angle is decreased. Thus, it was theorized that  $C_e$  would respond to changes in angle of inclination in a fashion similar to that depicted in Figure 5.

Angle (°)	<i>Vena contracta</i> location from crest (m)	Depth at <i>vena contracta</i> (m)	Contraction Coefficient $C_c$
90.00	0.075	0.204	0.669
71.57	0.070	0.209	0.688
56.31	0.061	0.210	0.690
45.00	0.058	0.219	0.718
26.57	0.030	0.211	0.692
14.04	0.015	0.197	0.647
0.00	0.000	0.155	0.508

Table 2: *Vena contracta* location and depth for various USBR inclined weir angles.

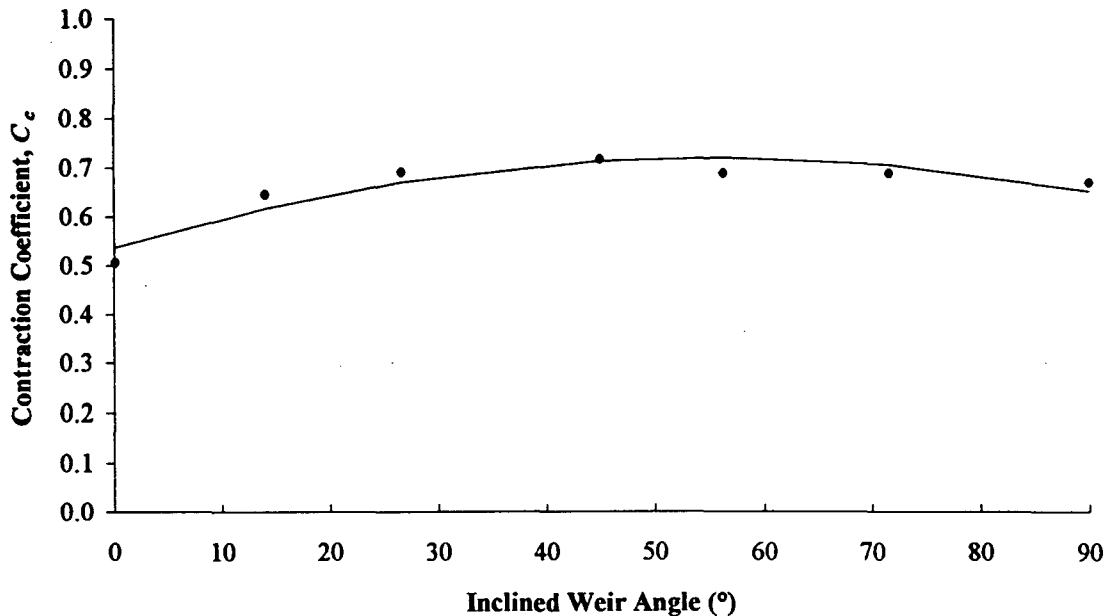


Figure 5:  $C_c$  as a function of USBR inclined weir angle.

### Submerged Weirs

When the tailwater in the canal rises above the crest of a sharp-crested weir, the weir becomes submerged. Under this condition, the discharge depends not only on the upstream head but also the downstream head,  $h_2$  (Brater and King, 1976). Generally, sharp-crested weirs are not used for flow measurement in the submerged state because the accuracy of the discharge measurements is reduced. However, the discharge characteristics of the overshot gate under submerged conditions should also be determined because the canal controlling aspects of the overshot gate may require the gate to operate in a submerged state. This can be done by assuming that the overshot gate also behaves like a sharp-crested weir under submerged conditions. Villemonte (1947) developed the following useful equation to estimate the discharge over a submerged rectangular sharp-crested weir:

$$Q = C_{df} Q_o = Q_o \left[ 1 - \left( \frac{h_2}{h_1} \right)^{1.5} \right]^{0.385} \quad [10]$$

where  $C_{df}$  = drowned flow reduction factor;  
 $Q_o$  = discharge under free-flow conditions with upstream head =  $h_1$ ;  
 $h_1$  = upstream head; and  
 $h_2$  = downstream head.

Villemonte recommended that the downstream head,  $h_2$ , be measured downstream from the disturbance created by the nappe [about 2 to 3 m (6 to 10 ft)] and that the tailwater basin be sufficiently wide to permit free circulation of the water underneath the nappe (Ackers et al, 1978). Villemonte (1947) claims that the drowned flow reduction factor for rectangular control sections can be determined to within 3% only if values of  $h_2/h_1$  are less than 1/3. Brater and King (1976) also point out that the accuracy of a sharp-crested weir is greatly reduced under submerged conditions and that some of the data obtained by Villemonte would have been better represented by a slightly different curve than the one given in Equation 10. They recommend individual weir calibrations if the accuracy required is greater than that provided by Villemonte's equation. For these laboratory experiments, Villemonte's drowned flow reduction factor was used in the following form:

$$C_{df} = A \left[ 1 - \left( \frac{h_2}{h_1} \right)^{1.5} \right]^n \quad [11]$$

where  $A$  and  $n$  are empirical constants.



## LABORATORY TESTS

Laboratory tests were performed on two different overshoot gates. The tests were performed in a glass-sided rectangular open channel that was 1.229 m (48-3/8 in) wide and 15 m (50 ft) long. Water was pumped from a large sump into a 3-m (10-ft) diameter constant head tank. From there the water entered the glass-sided channel through a series of baffles that were used to straighten the flow in the channel and to create a uniform flow profile. With no obstructions in the channel, a maximum flow rate of about 420 l/s (15 cfs) can be achieved. All flow rates were measured using a 25-ton weighing tank system, accurate to  $\pm 0.1\%$ .

A plan view of a typical overshoot gate installation in the laboratory can be seen in Figure 6. The side supports of the overshoot gate caused a side contraction in the water before it reached the crest. Because the contraction was made in the plane of the hinge line and the streamlines had a chance to straighten before they reached the crest, it was assumed that the leaf gate behaved as a suppressed weir ( $b_c/B_2 = 1$ ) regardless of the entrance contraction ratio ( $B_2/B_1$ ). A typical elevation view of an overshoot gate along with all the definitions of the pertinent dimensions appears in Figure 7.

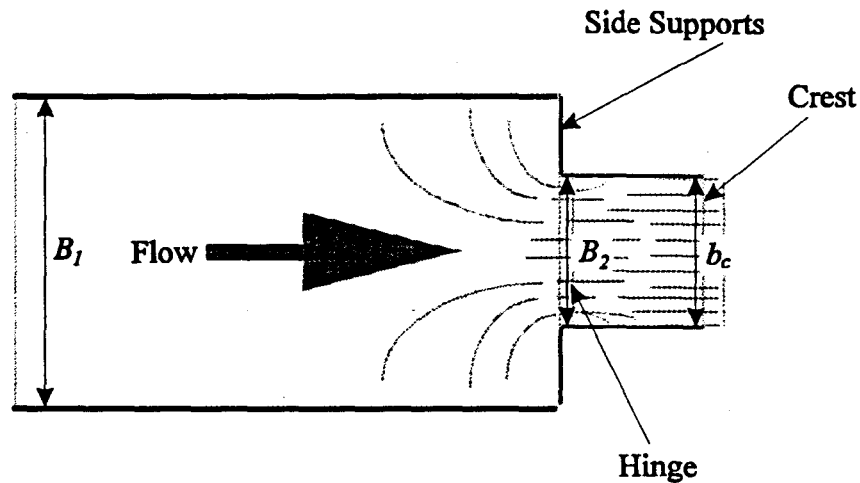


Figure 6: Plan view of leaf gate contraction.

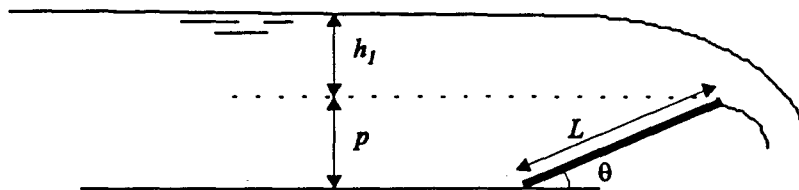


Figure 7: Elevation view of leaf gate.

The first gate studied was a full width weir that was shop-constructed at the US Water Conservation Laboratory (USWCL) in Phoenix, AZ, from 0.635-cm (1/4-in) thick aluminum. The width of the gate was 1.2 m (4.0 ft) while the length of the gate's blade was 0.61 m (2.0 ft). Because this gate had no side supports, there was no entrance contraction and  $b_c/B_1 = 1.0$ .

Structural aluminum angle 7.62 cm (3 in) thick was bolted to the underside of the leaf gate to limit the deflection under water loading. A 2.54-cm (1-in) aluminum rod was welded to the lower backside of the leaf gate and served as half of a hinge when set into a 2.54-cm (1-in) aluminum channel. This created a pivot that did not leak significantly. The aluminum channel was then welded to another 0.635-cm (1/4-in) sheet of aluminum which was then affixed and sealed to the laboratory channel floor using silicon sealant. The sides of the overshot gate were equipped with a J-type seal constructed from wooden dowel rods and gas pipe tape. The gate still leaked slightly, but it was determined that these small leaks did not significantly affect the calibration. The gate was raised and lowered by two steel cables that attached to the angle supports and wound onto a 2.54-cm (1-in) diameter steel-rod drum that could be rotated to achieve gate positioning. This drum assembly was supported on the metal frame of the glass-sided channel. A gear box was used to turn the steel rod which then wrapped the steel cables around itself and raised the gate. Because of the structural angle supports and the hinging system used, the gate angles were limited to between 23° and 39°. A schematic diagram of the USWCL gate is shown in Figure 8.

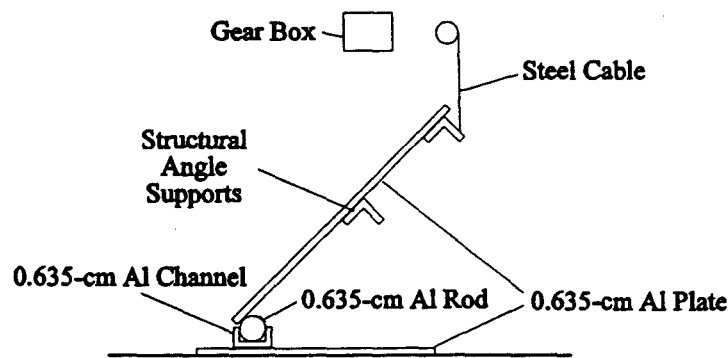


Figure 8: Schematic diagram of the USWCL overshot gate.

The second gate tested was a commercial version manufactured by Armtec, Inc. This gate was made of 0.318-cm (1/8-in) stainless steel plate and was 1.14 m (3.75 ft) wide and 0.46 m (1.5 ft) long. This gate had side supports and an entrance contraction ratio ( $B_2/B_1$ ) of 0.925. The configuration of the Armtec gate was similar to that of the USWCL gate. The hinge of the gate was a stainless steel piano hinge that was sealed with a rubber sheet. The hinging system on the Armtec gate was raised above the basic channel floor by mounting it on a 7.62-cm (3-in) square channel. This allowed the Armtec gate to be lowered to a horizontal position. The hoisting mechanism and the laboratory installation limited the maximum angle that could be achieved to around 65°. The sides were sealed with commercially available rubber J-seals and the leakage through the gate was minimal. This channel was then bolted to the same 0.635-cm (1/4-in) aluminum that was already sealed to the floor for the USWCL gate.

Free-flow tests were performed on both of these gates while submergence tests were performed on just the Armtec gate. For free-flow tests, a particular leaf gate angle and flow rate were selected and set in the laboratory. The gate angle was measured with a digital inclinometer that was accurate to  $\pm 0.1^\circ$ . The flow rate was measured using the weigh tank system. The upstream head on the gate was measured using a 0.6-m (2-ft) length of 2.54-cm (1-in) diameter steel pipe plugged on both ends and placed parallel to the flow about 1.2 m (4 ft) upstream of the base of the gate. Holes were drilled around the perimeter of the pipe at a section about 1/3 of the way from the downstream end and polyvinyl tubing was attached to a pressure tap located at the downstream end of the pipe. The tubing was then connected to a small movable stilling well that was located directly above the crest of the gate. Thus, the same point gage could be used to detect both the crest level and the upstream water surface without having to move the point gage. This method of head detection eliminated the translation error associated with moving the point gage.

A schematic diagram of the head detection system is shown in Figure 9. The head was measured at a variety of discharges for each angle. Six different angles were tested on the USWCL gate while 7 different angles were analyzed using the Armtec gate. False side walls were also installed to narrow the gate width to provide calibrations for different entrance contraction ratios ( $B_2/B_1$ ) for 3 different gate angles on the Armtec gate.

The submergence tests were performed similar to the free-flow tests. The upstream and downstream heads were measured using the method described earlier. In order to avoid the disturbance created by the plunging nappe, the downstream head was measured about 4.5 m (15 ft) downstream of the gate. The submergence ratio ( $h_2/h_1$ ) was controlled by another leaf gate that was located about 6 m (20 ft) downstream of the test gate. Because the tailwater surrounded the nappe on all three sides, the nappe was confined downstream of the overshoot gate and not allowed to circulate freely. This was not recommended by Villemonthe (1947) because regions of subnormal pressure will be introduced in the confined nappe and the same discharge will be passed over the gate at a lower head,  $h_1$ . Having a nappe confined downstream has a similar effect on submerged flow that an inadequately ventilated nappe has on unsubmerged flow. It is not clear how confining the nappe affects the calibration of the submerged overshoot gate. To perform the submergence test, a gate angle and flow rate were selected. After the system was calibrated under free-flow conditions, a limiting submergence ratio was determined by raising the downstream leaf gate until a change in the upstream head could be detected. From this point on, the downstream leaf gate was raised slightly and the corresponding upstream and downstream heads were recorded. This process was repeated until the leaf gate was about 95% submerged. No submergence tests were performed on the USWCL gate; however, 3 to 7 tests were performed on each of the angles tested on the Armtec gate. A summary of all the laboratory data taken during these experiments appears in Appendices III through VII.

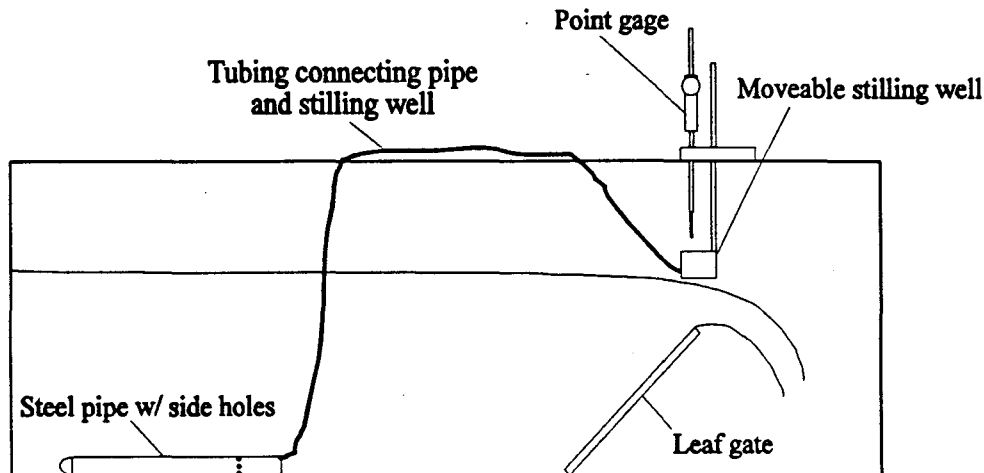


Figure 9: Schematic diagram of the head detection system.

## RESULTS

### Adjustments to the Discharge Equation

The blade on Armtec's gate was smooth and clean, but the edge was not perfectly sharp. The upstream corner of the gate had a slight rounding due to shearing the blade to size. This rounding had a radius of approximately 0.05 cm (0.02 in) and has the effect of increasing the discharge over the gate. To account for this, Schoder and Turner (1929) give an empirical expression for the increase of discharge due to rounding of the crest ( $C_r$ ). It was assumed that the rounding would have less of an effect on the flow rate as the gate angle was lowered. Thus, Schoder and Turner's  $C_r$  was modified as follows:

$$C_r = 1 + 0.0368 \frac{r}{h_1^{0.75}} \sin \theta \quad [12]$$

where  $C_r$  = coefficient to correct for rounding of the crest;  
 $r$  = radius of crest rounding in centimeters;  
 $h_1$  = head on gate in meters; and  
 $\theta$  = gate angle.

The side seals on the Armtec gate were so large that they affected the flow area over the crest. At high heads, the side seals did not affect the flow very much; however, at low heads, the cross-sectional seal area became a large percentage of the total flow area over the crest. To account for this, Equation 8 was modified by subtracting the seal area out of the flow area. The following equation is the form of the discharge equation that was used to calculate  $C_a$  from the laboratory experiments:

$$Q = C_a C_r C_e \frac{2}{3} \sqrt{2g} [(h_1 + K_h)(b_c + K_b) - 2A_s \cos \theta] \sqrt{h_1 + K_h} \quad [13]$$

where  $A_s$  = cross-sectional area of J-seal and all other terms are as previously defined (see Figure 7).

### Unsubmerged Gates

Only the calibrations for the Armtec gate were used in determining the empirical coefficients in the discharge equation. The calibrations from the USWCL were used simply to verify the results obtained from the Armtec gate. Values for  $C_a$  were calculated for each of the free-flow tests performed on the Armtec gate using Equation 13. The results of a typical calibration run appear in Figure 10.

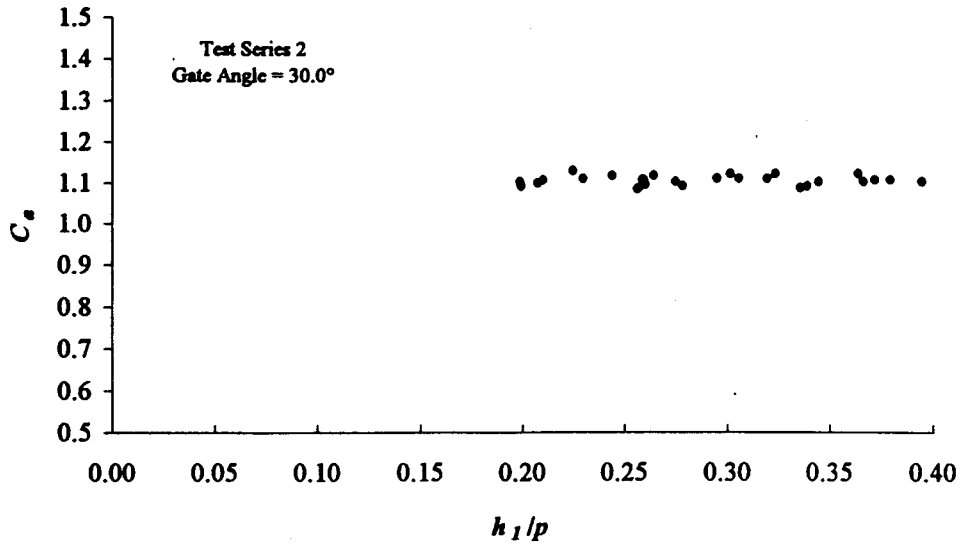


Figure 10: Values of  $C_a$  versus  $h_1/p$  for the Armtec gate at a 30.0° angle.

There is some scatter in  $C_a$ , but there does not appear to be a strong functional relationship between  $h_1/p$  and  $C_a$ . Thus, it was assumed that  $C_a$  was not dependent upon  $h_1/p$  and was a function of the gate angle only. The average value of  $C_a$  for a given angle was determined by performing a linear regression of the measured flow rate versus the theoretical flow rate given by the sharp-crested weir equation (Equation 4). The slope of the line obtained from this regression analysis will be the average  $C_a$  for that angle. An example of this analysis can be seen in Figure 11. The average values for  $C_a$  as well as the specific angles used for the Armtec gate tests appear in Table 3.

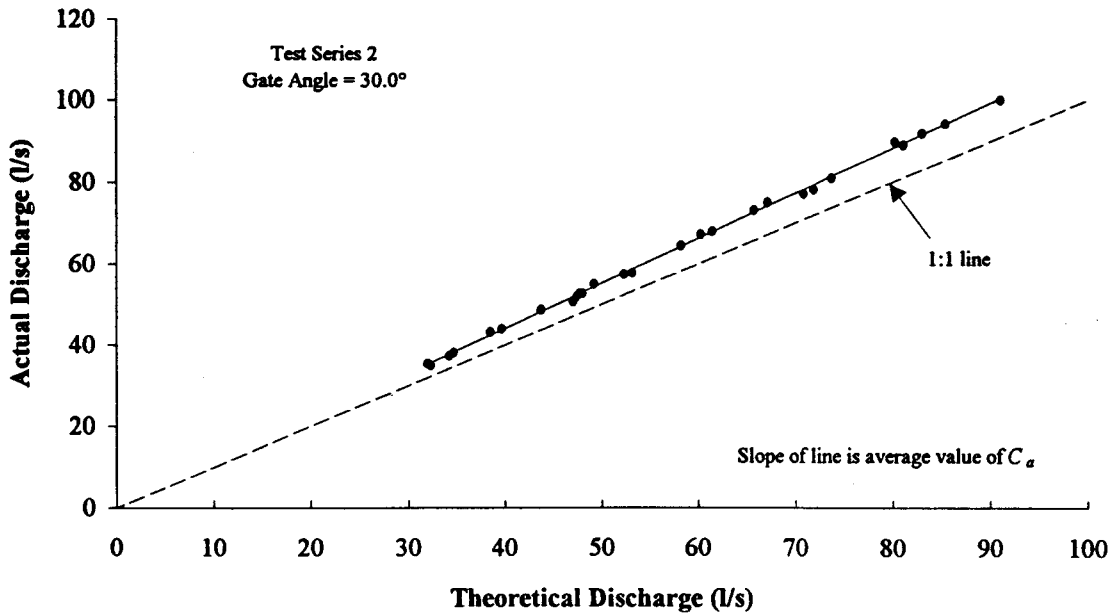


Figure 11: Actual discharge versus theoretical discharge for determination of  $C_a$ .

Gate Angle (°)	$C_a$	Number of Tests
16.2	1.081	15
22.4	1.101	25
30.0	1.106	28
36.4	1.116	35
43.6	1.115	8
54.2	1.108	35
63.4	1.097	14
90.0	1.000	By definition

Table 3: Average values of  $C_a$  for the Armtec gate at various angles.

The average values of  $C_a$  reported in Table 3 were plotted against the gate angle and can be seen in Figure 12. The shape of the solid portion of this curve can be approximated by a second-order polynomial with a maximum  $C_a$  value occurring at about 45°. This is very similar to the relationship of  $C_c$  versus angle of inclination as shown in Figure 5. A second order polynomial curve was empirically determined by applying a least-squares technique to the data. The following empirical equation was obtained:

$$C_a = 1.0333 + 0.003848\theta - 0.000045\theta^2 \quad [14]$$

where  $\theta$  = gate angle in degrees.

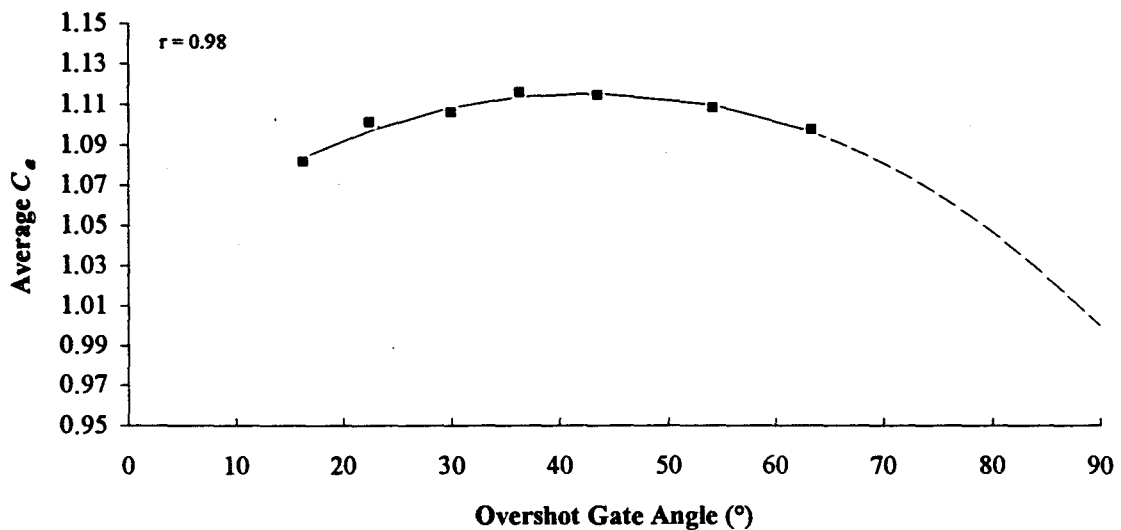


Figure 12: Average  $C_a$  values and empirical curve fit versus gate angle.

The Armtec gate was also analyzed for the effect of inserting the gate system into a wide channel as well as for changes in gate angle. Three different angles (36.4°, 54.2°, and 63.4°) were tested with different entrance contraction ratios. These side contractions were accomplished by making false walls on the weir plate at different widths to give hinge to main-channel width ratios ( $B_2/B_1$ ) as shown in Table 4. From the calibration results presented in Table 4,  $C_a$  does not appear to be a strong function of the entrance contraction ratio ( $B_2/B_1$ ). Thus, it was assumed that Equation 14 can be used to describe  $C_a$  for all values of  $B_2/B_1$ .

Gate Angle (°)	$B_2/B_1$	$C_a$	Number of Tests
36.4	0.925	1.116	13
	0.841	1.120	12
	0.586	1.110	10
54.2	0.925	1.107	14
	0.835	1.118	11
	0.506	1.110	10
63.4	0.925	1.101	7
	0.838	1.104	7

Table 4: Average values of  $C_a$  for different entrance contraction ratios and gate angles.

#### Submerged Gates

A summary of the various tests performed on the submerged Armtec gate appears in Table 5. The empirical coefficients  $n$  and  $A$  in Equation 11 were obtained using a least-squares curve fitting technique. A typical calibration data point set, a curve fit to the modified Villemonte equation, and a comparison with Villemonte's sharp-crested submerged weir equation (Equation 10) can be seen in Figure 13.

The modified Villemonte equation does not exactly fit the general shape of the test data that was collected, and a slightly different curve may describe the data more accurately. A similar observation was reported by Brater and King (1976) for submerged vertical sharp-crested weirs.

Gate Angle (°)	$q$ (l/s per m width)	$n$	$A$	Gate Angle (°)	$q$ (l/s per m width)	$n$	$A$
16.2	36.95	0.251	0.997	36.4	30.84	0.345	1.024
	60.08	0.229	1.020		37.24	0.339	1.029
	83.34	0.236	1.059		50.06	0.335	1.032
	121.53	0.229	1.068		66.55	0.318	1.035
22.4	37.60	0.292	1.024	43.6	23.74	0.354	1.004
	51.58	0.284	1.036		30.47	0.352	1.007
	67.36	0.287	1.051		37.60	0.356	1.026
	89.26	0.263	1.046		45.50	0.336	1.018
	109.96	0.247	1.049		64.03	0.333	1.026
	130.79	0.251	1.058		78.01	0.316	1.029
30.0	132.67	0.249	1.060	54.2	18.74	0.381	0.994
	30.83	0.318	1.030		29.91	0.387	1.001
	48.04	0.311	1.047		37.56	0.362	1.005
	63.86	0.326	1.052				
	80.42	0.301	1.052				

Table 5: Values of  $n$  and  $A$  for various gate angles and specific discharges,  $q$ .

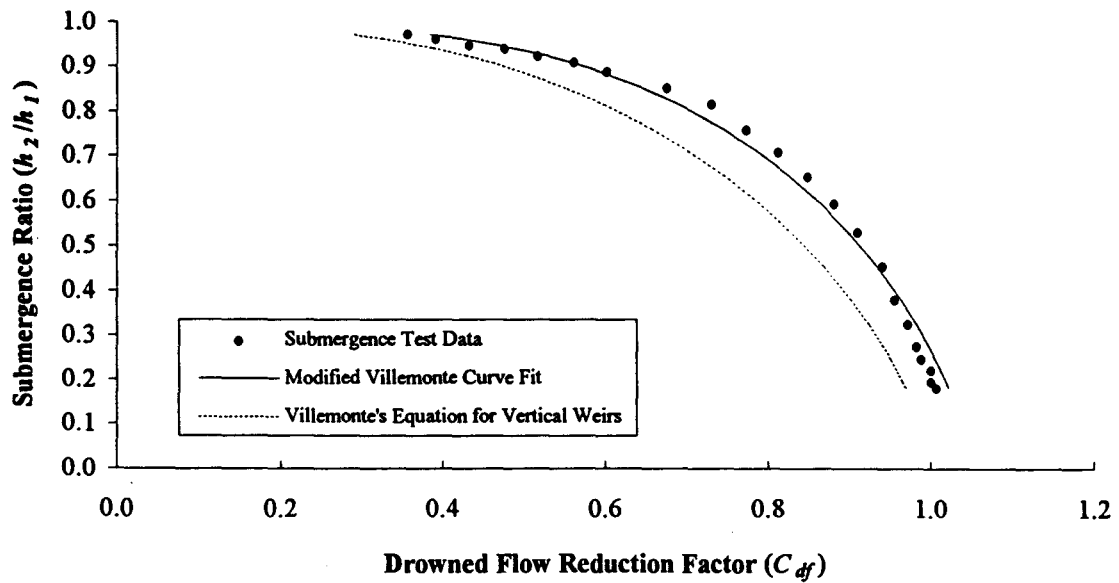


Figure 13: Typical calibration curve for submerged Armttec overshoot gate.

Tests were also performed on contracted submerged gates. These tests were performed on only a few of the angles and a summary of these results appears in Table 6. There does not appear to be any real pattern to the changes of  $n$  and  $A$  with entrance contraction ratio ( $B_2/B_1$ ) and discharge. Thus, the data for both the full-width and contracted gates were combined for the remaining analysis.

Gate Angle (°)	$B_2/B_1$	$q$ (l/s per m width)	$n$	$A$
54.2	0.508	32.05	0.366	0.998
	0.508	45.08	0.348	0.999
	0.508	64.49	0.342	0.991
	0.839	26.68	0.370	1.002
36.4	0.839	46.40	0.357	1.007
	0.588	79.58	0.311	1.023
	0.844	23.96	0.336	0.995
	0.844	41.29	0.310	1.014
	0.844	64.73	0.304	1.033
	0.844	97.10	0.280	1.032

Table 6: Values of  $n$  and  $A$  for submerged Armtec overshoot gate at various entrance contraction ratios and specific discharges.

The values of  $n$  and  $A$  depend upon both discharge and gate angle as illustrated in Figures 14 and 15. As the gate angle increases, the calibration curve approaches the shape defined by Villemonte's equation for vertical sharp-crested weirs (Figure 15). Also, the shape of the calibration curves were slightly influenced by the discharge. In Figure 14, tests performed at low discharges were generally closer to Villemonte's equation for vertical weirs than tests performed at high flow rates. However, The dependence of the values of  $n$  and  $A$  upon the discharge is not strong, and it was assumed that they are a function of gate angle only. Using the average values of  $n$  and  $A$  at each gate angle, the following empirical equations can be developed:

$$n = 0.1525 + 0.006077\theta - 0.000045\theta^2 \quad [15]$$

$$\begin{aligned} A &= -0.0013\theta + 1.0663 && \text{for } \theta < 60^\circ \\ A &= 1.0 && \text{for } \theta > 60^\circ \end{aligned} \quad [16]$$

where  $\theta$  = gate angle in degrees.

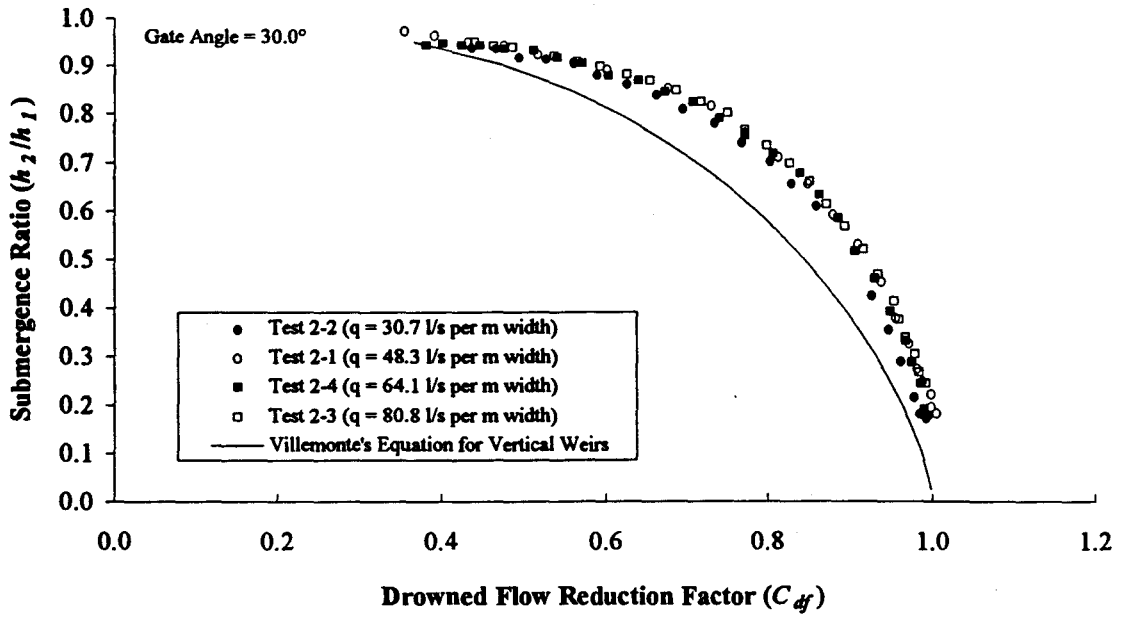


Figure 14: Typical calibrations for the submerged Armttec leaf gate (one angle, various discharges).

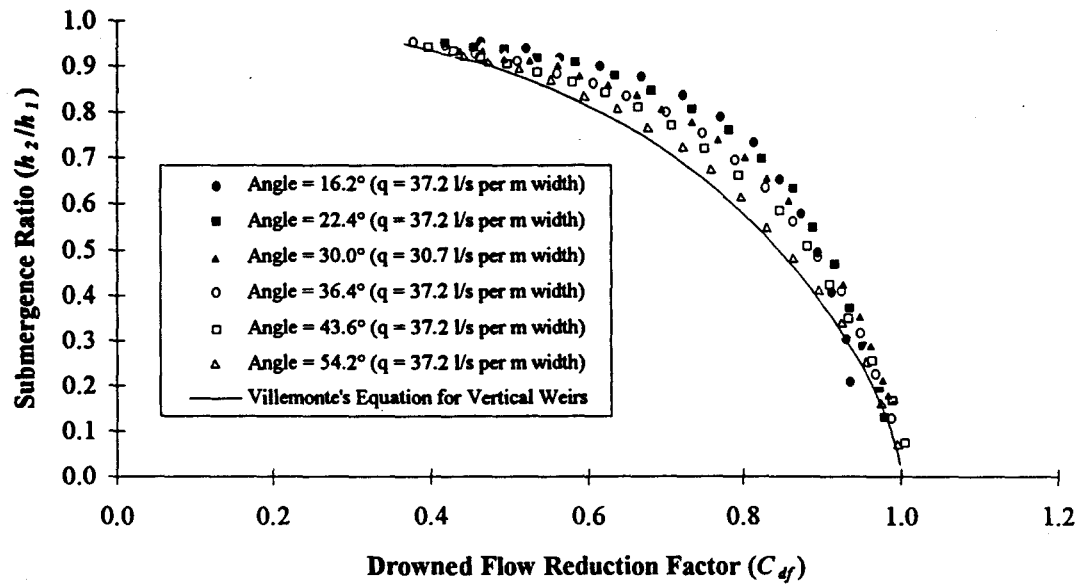


Figure 15: Typical calibrations for the submerged Armttec leaf gate (various angles, similar discharges).

## DISCUSSION OF RESULTS

### Unsubmerged Gates

The general shape of the  $C_a$  versus gate angle curve in Figure 12 is very similar to the  $C_c$  versus angle of inclination curve in Figure 5. Both of these curves appear to have a maximum around a  $45^\circ$  angle of inclination. By definition,  $C_a$  was assumed to pass through 1.0 for a vertical weir. However, because the Armtec leaf gate could not be raised to the vertical position, it was not possible to determine if  $C_a$  approached 1.0 at higher angles.

It was also not possible to determine the behavior of  $C_a$  at very low gate angles because the downstream tailwater prevented the gate from being properly ventilated at angles lower than about  $15^\circ$ . Equation 14 does not predict the behavior of the leaf gate at very high angles or very low angles since tests were not performed in those areas. Equation 14 will only accurately describe the behavior of  $C_a$  between the angles of  $16.2^\circ$  and  $63.4^\circ$  and should not be used outside these limits.

### Comparisons to Other Experiments

The accuracy of Equation 14 was determined by comparing it to four different data sets: data from the USWCL leaf gate tests, data from experiments by the US Bureau of Reclamation (USBR, 1948), data from experiments by Bazin (USBR, 1948), and data from field experiments performed in the IID.

*Experiments on the USWCL gate*--The USWCL gate was calibrated using the method described earlier. Unlike the Armtec gate, the USWCL leaf gate had no side supports or contractions ( $b_c = B_1 = B_2$ ). The USWCL gate also had a very sharp edge, so no correction for crest rounding was needed. Also, the edge seals did not affect the flow area over the crest and no correction was needed for the seal area. The actual discharge was over predicted by Equations 8 and 14 by an average of 0.80% with a standard deviation of 1.67% as can be seen in Figure 17. A summary of the data taken for the USWCL gate tests appears in Appendix VII.

*Experiments of the USBR*--In the USBR's final report on the Boulder Canyon Project (1948), data from similar experiments on full-width weirs with sloping faces were listed. The experiments were performed in a channel that was 5.5 m (18 ft) long, 2.9 m (9.4 ft) deep, and 0.61 m (2 ft) wide. The channel also had a moveable floor so different gate heights,  $p$ , could be obtained. Gravel baffles were introduced at the beginning on the channel to evenly distribute the approaching flow. Heads were measured using a hook gage in a stilling well connected to a piezometer in the floor 3.0 m (9.9 ft) upstream of the weir. The discharges were measured using Venturi meters. The stainless steel weirs used in these experiments were 0.79 cm (0.31 in) thick and were machined at an angle of  $50^\circ$  in order to form a knife-like edge. The width at the top of the blade was only 0.159 cm (1/16 in) thick.

These experiments were performed to determine the profile of the upper and lower nappes of ogee dams with inclined upstream faces. The USBR performed tests on three different gate angles:  $71.57^\circ$ ,  $56.31^\circ$ , and  $45.00^\circ$ . These tests were performed over a wide range of  $h_1/p$  (as high as 14 in some cases). Since all the tests done in the laboratory had  $h_1/p$  values less than 1.0, only data from the USBR tests with  $h_1/p$  less than 1.0 were considered. Also, the  $71.57^\circ$  experiments were not considered because an angle this high was not tested in the laboratory and would be out of the range for which Equation 14 is defined. The discharge calculated from Equations 8 and 14 over predicts the USBR's measurements by an average error of 0.54% and a standard deviation of 0.99% (see Figure 17). A summary of the USBR's experiments on inclined weirs appears in Appendix IX.

*Experiments of Bazin*--Bazin performed his experiments between 1886 and 1887 in France on full-width, thin-plate weirs. Measurements were taken in a channel that was 213 m (700 ft) long and 2.00 m (6.56 ft)

wide. The weirs were made of iron that was 0.70 cm (0.276 in) thick and "carefully straightened." For his first 3 tests, Bazin measured the discharges volumetrically.

After that, he calibrated the other weirs by comparing them to the first 3 "reference" weirs. The head was measured using a hook gage in a stilling well connected to a large piezometric tap that was 5.0 m (16.4 ft) upstream of the weir. Although "... Bazin's instrumentation was good and his technique was meticulous" (Kindsvater and Carter, 1959), his results differ from most other investigators. Questions have been raised as to whether the crests in Bazin's experiments were truly straight or sharp (Schoder and Turner, 1929).

The USBR's Boulder Canyon Project Final Report (1948) also presented some of the data from experiments performed by Bazin on weirs with sloping faces. Apart from the angles studied by the USBR, Bazin also performed experiments on gate angles of 26.57° and 14.04°. All of Bazin's data had  $h_1/p$  values that were either near or below 1.0. Thus, all his data was used for comparison except for the data from the 71.57° angle tests. Equations 8 and 14 under predicted Bazin's data by an average 3.48% with a standard deviation of 2.29% (see Figure 17). Bazin's data on inclined weirs is summarized in Appendix VIII.

*Field Experiments*--Field experiments were also carried out in the IID during the summer and fall of 1993. Two sites were tested during these experiments. The first leaf gate was located on the Plum Canal and had a 1.55 m (5.08 ft) long blade. The second leaf gate was located on the Oasis Canal and had a 1.70 m (5.58 ft) long blade. Both of these overshot gates had widths of 1.63 m (5.35 ft). The Plum Canal was a trapezoidal concrete-lined channel with a bottom width of 0.61 m (2.0 ft) and side slopes of 1.5 to 1. The Oasis Canal was also a trapezoidal concrete-lined canal with a 0.61 m (2.0 ft) bottom width; however, its side slopes were 1.25 to 1. A schematic diagram of a portion of the Oasis Canal along with the test-site location appears in Figure 16. These tests were performed differently than those in the lab. In the field, the flow rate was held constant and a variety of angles were calibrated instead of holding the angle constant and varying the flow rate. This was done because of the difficulty of changing the flow rate in the field canals. The upstream head was measured by the same method used in the laboratory. The flow rate in the canal was measured using a computer calibrated broad-crested weir that was accurate to within  $\pm 2\%$ . Care had to be taken to ensure that the gate was properly ventilated in the field. At angles less than 20°, the overshot gate became only partially ventilated and this led to large errors in the discharge prediction. These points were not included in the data analysis. The crest of the field gate was slightly rounded and the edge seals affected the flow area in a manner similar to the Armtec laboratory overshot gate. However, the heads were so high in the field that the small corrections made by including these effects were negligible. Thus, the following equation was used to calculate the discharge for the field experiments:

$$Q = C_a C_e \frac{2}{3} \sqrt{2g} (b_c + K_b)(h_1 + K_h)^{1.5} \quad [17]$$

The relative heads,  $h_1/p$ , in all the experiments were less than 0.7, thus Equation 14 can be used to describe  $C_e$ . As would be expected, the data of the field experiments was more scattered than any of the laboratory experiments. Using Equation 17, the field discharge was under predicted with an average error of 6.39% and a standard deviation of 3.16% (see Figure 17). There was a difference between the tests performed on the Plum Canal and the tests performed on the Oasis Canal. The calibrations on the Plum Canal alone had an average error of around 2.2% while the calibrations on the Oasis Canal alone had an average error around 7.3%. The field data is summarized in Appendix X.

The point gage and moveable stilling well system used to detect the head on the overshot gate is accurate to within 1%. This leads to a maximum error in discharge due to errors in head measurements of 1.5%. There are many other sources of error that can be identified in relating the leaf gate calibration in the field to the calibration performed on the Armtec gate in the laboratory. A summary of the possible systematic errors can be seen in Table 7.

The broad-crested weir used for the determination of the flow rate in the field has an error of  $\pm 2\%$ . The gate leaked slightly through the side J-seals and the estimated error was 0.5%. Also, the crest of the leaf gate was not perfectly level. There was approximately a 1 cm (0.4 in) drop in the leaf gate crest across its width.

For the flows and heads encountered in the field, the use of the average head on the gate in the discharge calculations will lead to an error of about 0.25% (Horton, 1907). Because the blade in the field was longer and rougher than the one studied in the laboratory, an error of approximately 0.5% may be introduced due to additional friction losses.

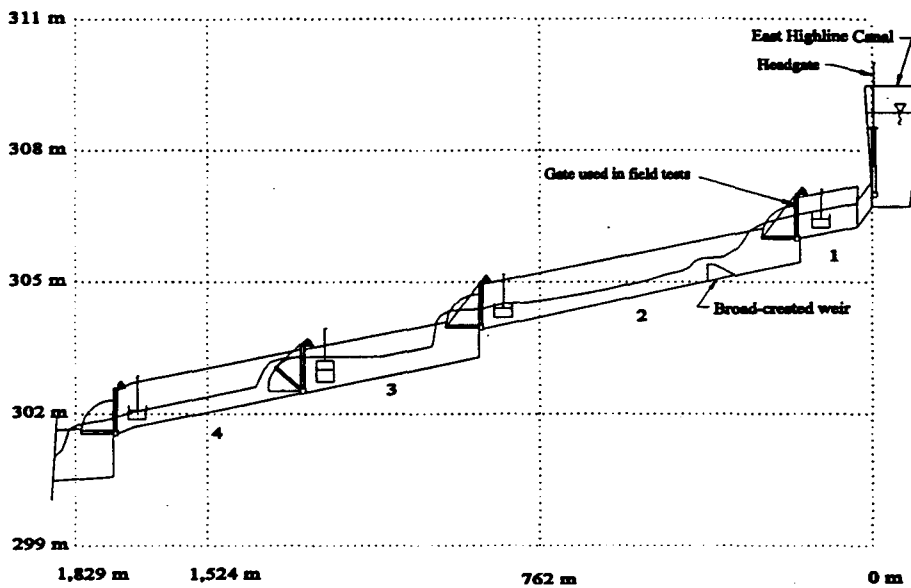


Figure 16: Schematic diagram of Oasis Canal and location of field tests.

Of all the errors presented in Table 7, the error for the distribution of the velocity of approach is the most difficult to estimate. Schoder and Turner (1929) found in their tests that the calibration of sharp-crested weirs could vary as much as 26% simply by adjusting the velocity distribution approaching the weir. Variations in the distribution of the velocity of approach may be able to explain the differences between the calibrations on the Plum and Oasis Canals. About 8 m (25 ft) upstream of the leaf gate on the Oasis Canal there was a slight contraction in the channel geometry. This contraction had a noticeable effect on the water surface, especially at low water depths. Also, the contraction from the trapezoidal approach channel to the rectangular leaf gate control section appeared to be more streamlined in the Plum Canal than in the Oasis Canal. These two factors may have disturbed the distribution of the velocity of approach in the Oasis Canal enough that an approximate error of 3% was introduced.

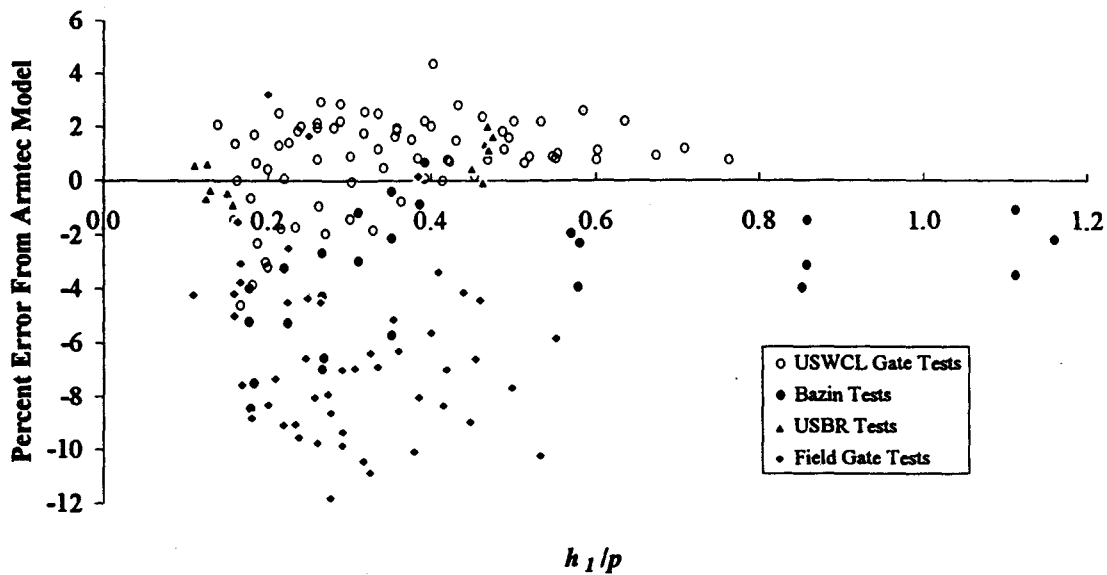


Figure 17: Percent error of various leaf gate tests.

Source of Error	Magnitude of Error
Head detection	1.5%
Comparison flume	2%
Gate leakage	0.5%
Plate roughness	0.5%
Distribution of velocity of approach	3%
Inclination of crest	0.25%

Table 7: Sources of systematic error in the calibration of the field leaf gate.

### Submerged Gates

A modified version of the Villemonte equation was used to describe the drowned flow reduction factor for the Armttec overshoot gate. Different entrance contraction ratios ( $B_2/B_1$ ) did not appear to affect the values of  $n$  or  $A$  in Equation 11. Equations 11, 15, and 16 can be used to describe the drowned flow reduction factor of the Armttec gate with an average error of -0.11% and a standard deviation of 4.08%. The high standard deviation is a result of Equation 11's inability to perfectly follow the data points from the submergence calibrations (see Figure 13). Brater and King (1976) also report that Villemonte's equation did not exactly fit the data obtained from vertical sharp-crested weirs. Thus, if a high degree of accuracy is needed, Brater and King (1976) recommend that each particular gate be tested in a laboratory under conditions similar to those in the field.

No literature was available for calibration tests done on submerged inclined sharp-crested weirs and no submergence tests were performed on the USWCL gate. However, tests were performed in the field. These tests were carried out in a manner similar to those done in the laboratory; however, only a limited number of submergence ratios were obtained because of the difficulty in controlling the downstream water surface.

Like the unsubmerged case, the errors due to rounding of the crest and interference from the side seals of the submerged gate are negligible because of the large heads encountered in the field. The following equation was used to calculate the discharge for a submerged overshot gate in the field:

$$Q = C_{df} C_a C_e \frac{2}{3} \sqrt{2g} (b_c + K_b)(h_1 + K_h)^{1.5} \quad [18]$$

Using Equation 14 to describe  $C_a$  and Equations 11, 15, and 16 to describe  $C_{df}$ , the field results were predicted with an average error of 3.99% and a standard deviation of 1.07%. Tests were performed on a leaf gate on the Oasis Canal with an angle of 22.2° and a flow rate of 357 l/s (12.6 cfs). Submergence ratios ( $h_2/h_1$ ) from 0.15 to 0.65 were covered by the tests. Submergence tests performed at other gate angles and flow rates could not be completed because of the capacity limitations of the downstream canal. A comparison of the submerged field gate with submergence tests performed in the laboratory on the Armtec gate under similar conditions can be seen in Figure 18. A summary of the submerged data taken in the field appears in Appendix XI.

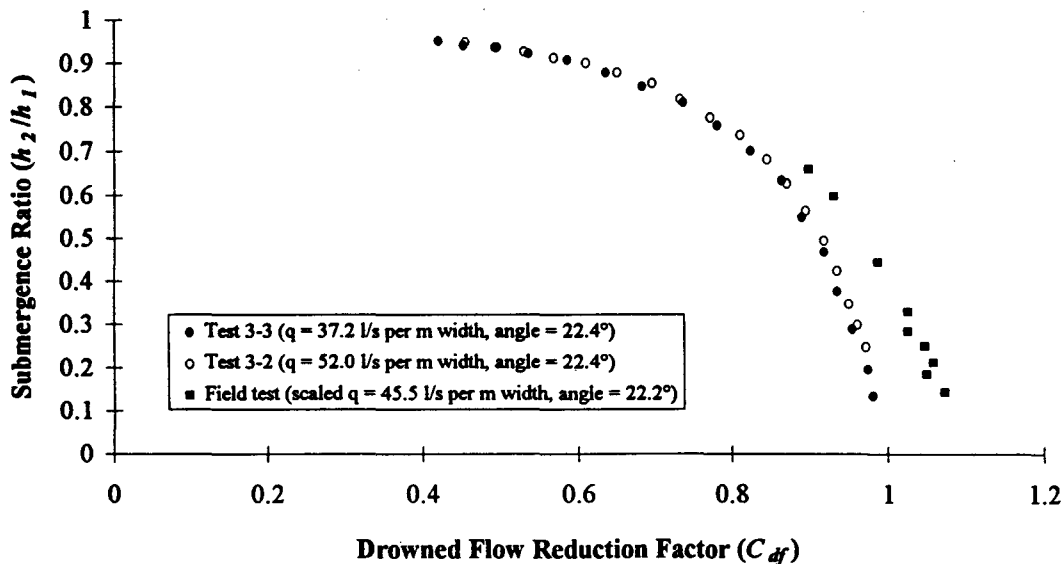


Figure 18: Comparison of field submergence tests to similar laboratory submergence tests.

It is surprising that the field submergence tests had a higher degree of accuracy than the free-flow tests because operating weirs under submerged conditions usually reduces their accuracy. It is felt that this result is fortuitous and resulted from the cancellation of different systematic errors. There are two reasons that might explain why the field tests performed better under submerged conditions than under free-flow conditions. First, since only one gate angle, one flow rate, and a limited number of submergence ratios were tested, it is difficult to say whether this trend will persist with other gate angles and discharges. Second, in the field, the nappe was allowed to circulate freely after it passed over the crest because there was a sharp drop in the channel bottom just downstream of the gate and the channel expanded from a rectangular control section to a trapezoidal section. These large expansions permitted the tailwater to circulate freely under field conditions as recommended by Villemonte (1947). However, in the laboratory, the tailwater was confined.

A confined downstream section introduces areas of low pressure and has the same effect on a submerged weir that an inadequately ventilated nappe has on a free-flow weir. Thus, the Armtec gate tested under the confined laboratory conditions was discharging water at a lower head than it would if the downstream channel permitted proper circulation of the water. This improper circulation of the water would cause a rise in the value of the drowned flow reduction factor. All the drowned flow reduction factors obtained from the laboratory experiments would then be higher than the ones obtained from the field experiments. Because Equations 14 and 17 under predict the discharges under free-flow conditions, a larger value of  $C_{df}$  should improve the accuracy of Equation 18 under submerged conditions. Since the conditions in the laboratory do not exactly mirror the conditions in the field, the actual accuracy of Equation 18 is not clear. Based on the performance of the unsubmerged gates in the field and the behavior of vertical weirs under submerged conditions, it is speculated that the discharge over a submerged leaf gate can be determined to within roughly 10%.

For overshot gates to predict the flow under submerged conditions, the downstream depth must be accurately determined. In many of the gates observed in the IID, no downstream depth measurement was possible because the flow entered a pipe immediately after the gate. In these cases, the overshot gate cannot be used to measure the discharge under submerged conditions because no downstream depth can be obtained. The ideal spot for measuring the downstream depth is past the disturbance created by the plunging nappe. Usually about 2 to 3 m (6 to 10 ft) downstream of the gate is an appropriate distance (Villemonthe, 1947). Because of the limited number of locations where a downstream depth can be measured in the IID and the small number of field calibrations performed, it is not recommended to use leaf gates to predict discharge when they are under submerged conditions.

## CONCLUSIONS

1. Equations 14 and 17 can be used to accurately describe the flow rate in the field of a properly ventilated free-flow leaf gate to within approximately 6.4% with a standard deviation of around 3.2%. These equations are valid for values of  $h_1/p$  less than 1.0 and for gate angles between  $16.2^\circ$  and  $63.4^\circ$ .
2. Equations 11, 15, 16 and 18 can be used to predict the discharge of a submerged overshot gate to within an apparent 4% based on limited field tests. However, because the laboratory and field tests did not have similar downstream conditions, it is felt that 10% is a more reasonable estimate of the accuracy of equations 11, 15, 16 and 18. These empirical equations are valid for values of  $h_1/p$  less than 1.0, gate angles between  $16.2^\circ$  and  $63.4^\circ$ , and submergence ratios less than 0.90
3. The drowned flow reduction factor predicted by Equations 11, 15, and 16 is larger than it should be because of the confined downstream channel section in the laboratory.
4. Different entrance contraction ratios ( $B_2/B_1$ ) do not affect the value of  $C_a$  because of the distance between the crest and the initial contraction at the hinge. This is true under both free-flow and submerged conditions.
5. Equation 11 does not perfectly describe the drowned flow reduction factor for a submerged gate. Individual calibrations are recommended if a higher accuracy is required.
6. It is speculated that the distribution of the velocity of approach has a major effect on the accuracy of Equations 14 and 17.
7. Only those sites where an appropriate downstream water depth can be obtained are suitable for flow measurement under submerged conditions.

## APPENDIX L REFERENCES

- Ackers, P., White, W.R., Perkins, J.A., and Harrison, A.J. (1978). *Weirs and Flumes for Flow Measurement*. John Wiley & Sons, New York. 316 pp.
- Bos, M.G. (1989). *Discharge Measurement Structures*. Publication No. 20, 3rd ed. International Institute for Land Reclamation and Improvement, Wageningen, The Netherlands. 401 pp.
- Brater, E.F., and King, H.W. (1976). *Handbook of Hydraulics*. 6th ed. McGraw-Hill, New York. 584 pp.
- Horton, Robert E. (1907). *Weir Experiments, Coefficients, and Formulas*. Water-Supply and Irrigation Paper No. 200, US Geological Survey, 195 pp.
- Kindsvater, C.E., and Carter, R.W. (1959). "Discharge Characteristics of Rectangular Thin-Plate Weirs." *Trans. Am. Soc. Civil Engrs.*, Vol. 124, p. 772-822.
- "Overshot Gate: Simple but Effective." (August, 1990). *Municipal and Industrial Water and Pollution Control*, Vol. 128, p. 21-22.
- Rouse, Hunter. (April, 1936). "Discharge Characteristics of the Free Overfall." *Civil Engineering*, Vol. 6, p. 257-260.
- Schoder, E.W., and Turner, K.B. (1929). "Precise Weir Measurements." *Trans. Am. Soc. Civil Engrs.*, Vol. 93, p. 999-1110.
- USBR. (1948). *Studies of Crests for Overfall Dams*. Bulletin 3. Boulder Canyon Project, Final Report. US Bureau of Reclamation, US Dept. of Interior, Denver, CO. 186 pp.
- Villemonite, J.R. (December 25, 1947). "Submerged Weir Discharge Studies." *Engineering News Record*, p. 866-869.



## APPENDIX II. GLOSSARY

- $A$  = empirical constant used in determining the drowned flow reduction factor;
- $A_s$  = cross-sectional area of gate side seals;
- $b$  = empirical constant used in determining the effective discharge coefficient;
- $b_c$  = width of the overshoot gate;
- $b_e$  = effective overshoot gate width;
- $B_1$  = width of the approach channel;
- $B_2$  = width of overshoot gate at hinge section;
- $C_a$  = gate angle correction coefficient;
- $C_c$  = contraction coefficient;
- $C_d$  = discharge coefficient for a sharp-crested weir;
- $C_d$  = drowned flow reduction factor;
- $C_e$  = effective discharge coefficient based on measured head;
- $C_r$  = crest rounding correction coefficient;
- $d$  = thickness of the *vena contracta*;
- $g$  = gravitational acceleration;
- $h_1$  = measured upstream head;
- $h_2$  = measured downstream head;
- $h_e$  = effective upstream head;
- $K_b$  = width adjustment factor to account for viscosity and surface tension;
- $K_h$  = head adjustment factor to account for viscosity and surface tension;
- $L$  = length of the blade of the overshoot gate;
- $m$  = empirical constant used in determining the effective discharge coefficient;
- $n$  = empirical constant used in determining the drowned flow reduction factor;
- $p$  = gate height;
- $q$  = discharge per unit width;
- $Q$  = discharge;
- $Q_o$  = discharge under free-flow conditions;
- $r$  = radius of crest rounding in centimeters;
- $v$  = velocity;
- $y$  = height of an arbitrary point above the weir crest;
- $y_c$  = critical depth; and
- $\theta$  = gate angle in degrees.



**APPENDIX III. DATA FOR FREE-FLOW ARMTEC OVERSHOT GATE**

**Test series #2**

Test dates: July 7, 8, 9, and 12, 1993  
Gate angle: 28.6°

Run #	Head (mm)	Discharge (l/s)	Head (ft)	Discharge (cfs)
2	78.9	50.87	0.259	1.796
3	85.6	58.01	0.281	2.049
4	93.0	67.42	0.305	2.381
5	103.3	77.07	0.339	2.722
6	112.8	89.21	0.370	3.150
7	121.6	100.32	0.399	3.543
8	104.2	78.38	0.342	2.768
9	106.1	81.15	0.348	2.866
10	112.2	89.94	0.368	3.176
11	116.7	94.40	0.383	3.334
12	99.7	75.13	0.327	2.653
13	94.2	68.23	0.309	2.409
14	90.8	64.55	0.298	2.279
15	84.7	57.71	0.278	2.038
17	80.2	52.66	0.263	1.860
18	70.7	44.10	0.232	1.557
19	64.0	37.58	0.210	1.327
20	79.6	52.47	0.261	1.853
21	75.3	48.85	0.247	1.725
22	69.2	43.31	0.227	1.530
23	64.6	38.30	0.212	1.353
24	61.6	35.14	0.202	1.241
25	79.2	51.38	0.260	1.814
26	79.9	52.94	0.262	1.870
27	81.4	54.94	0.267	1.940
28	61.3	35.28	0.201	1.246
29	114.6	91.97	0.376	3.248
30	98.5	73.02	0.323	2.579

**Test series #3**

Test dates: July 20 and 21, 1993  
Gate angle: 22.4°

Run #	Head (mm)	Discharge (l/s)	Head (ft)	Discharge (cfs)
1	101.2	74.89	0.332	2.645
2	107.9	83.49	0.354	2.948
3	114.3	91.09	0.375	3.217
4	120.4	98.96	0.395	3.495
5	128.3	109.28	0.421	3.859
6	141.7	128.03	0.465	4.521
7	149.0	138.52	0.489	4.892
8	155.8	148.35	0.511	5.239
9	162.2	157.67	0.532	5.568
10	169.8	169.96	0.557	6.002
11	96.0	69.82	0.315	2.466
12	89.0	61.47	0.292	2.171
13	86.0	58.33	0.282	2.060
14	82.6	54.96	0.271	1.941
15	78.0	50.24	0.256	1.774
16	72.5	44.78	0.238	1.582
17	66.4	39.03	0.218	1.378
18	61.3	34.52	0.201	1.219
19	157.6	149.57	0.517	5.282
20	87.2	58.98	0.286	2.083
21	70.7	43.00	0.232	1.518
22	103.3	77.02	0.339	2.720
23	123.7	102.08	0.406	3.605
24	141.4	125.73	0.464	4.440
25	159.1	151.71	0.522	5.357

**Test series #4**

Test date: July 29, 1993  
Gate angle: 36.4°

Run #	Head (mm)	Discharge (l/s)	Head (ft)	Discharge (cfs)
1	85.3	59.19	0.280	2.090
2	93.6	67.90	0.307	2.398
3	101.2	76.56	0.332	2.704
4	78.9	52.44	0.259	1.852
5	71.6	45.15	0.235	1.595
6	66.4	40.33	0.218	1.424
7	62.2	36.47	0.204	1.288
8	57.3	32.11	0.188	1.134
9	52.1	27.86	0.171	0.984
10	84.1	57.25	0.276	2.022
11	61.0	35.27	0.200	1.246
12	101.5	76.09	0.333	2.687
13	69.2	42.58	0.227	1.504

**Test series #5**

Test date: August 4, 1993  
Gate angle: 16.2°

Run #	Head (mm)	Discharge (l/s)	Head (ft)	Discharge (cfs)
1	124.1	103.10	0.407	3.641
2	133.8	114.84	0.439	4.056
3	141.7	127.58	0.465	4.506
4	153.3	143.82	0.503	5.079
5	164.3	160.78	0.539	5.678
6	114.3	90.90	0.375	3.210
7	103.9	78.46	0.341	2.771
8	94.8	67.58	0.311	2.387
9	84.7	57.08	0.278	2.016
10	76.8	48.71	0.252	1.720
11	67.7	39.83	0.222	1.406
12	54.3	28.08	0.178	0.992
13	118.3	95.30	0.388	3.366
14	150.3	138.98	0.493	4.908
15	62.2	34.49	0.204	1.218

**Test series #6**

Test date: August 12 and 13, 1993

Gate angle: 43.6°

Run #	Head (mm)	Discharge (l/s)	Head (ft)	Discharge (cfs)
1	69.8	41.83	0.229	1.477
2	77.7	49.43	0.255	1.746
3	87.8	60.10	0.288	2.122
4	98.5	71.28	0.323	2.517
5	116.4	92.22	0.382	3.257
6	126.5	104.69	0.415	3.697
7	141.1	124.15	0.463	4.384
8	81.3	34.69	0.201	1.225
9	53.6	28.26	0.176	0.998
10	48.2	23.93	0.158	0.845
11	62.2	35.29	0.204	1.246
12	75.3	47.51	0.247	1.678
13	93.3	66.35	0.306	2.343
14	112.8	88.96	0.370	3.142
15	131.1	112.74	0.430	3.981
16	98.8	73.22	0.324	2.586
17	78.9	52.03	0.259	1.837
18	60.7	33.85	0.199	1.195
19	112.2	89.20	0.368	3.150
20	69.2	43.00	0.227	1.518
21	60.7	34.84	0.199	1.230
22	52.1	27.92	0.171	0.986
23	51.5	27.15	0.169	0.959

**Test series #7**

Test date: September 3, 1993

Gate angle: 54.2°

Run #	Head (mm)	Discharge (l/s)	Head (ft)	Discharge (cfs)
2	83.5	56.37	0.274	1.991
3	96.0	69.50	0.315	2.455
4	102.7	77.08	0.337	2.722
5	111.6	87.38	0.366	3.086
6	78.9	51.93	0.259	1.834
7	70.1	43.32	0.230	1.530
8	62.8	36.86	0.206	1.302
9	54.9	30.08	0.180	1.062
10	48.8	25.18	0.160	0.889
11	42.7	20.57	0.140	0.727
12	60.0	34.20	0.197	1.208
13	71.6	44.57	0.235	1.574
14	69.8	42.95	0.229	1.517
15	44.2	21.42	0.145	0.757

**Test series #8**

Test date: December 28, 1993

Gate angle: 63.4°

Run #	Head (mm)	Discharge (l/s)	Head (ft)	Discharge (cfs)
8	89.3	62.22	0.293	2.197
9	75.3	48.22	0.247	1.703
10	70.7	43.57	0.232	1.539
11	57.9	32.39	0.190	1.144
12	50.3	26.28	0.165	0.928
13	44.5	21.97	0.146	0.776
14	35.4	15.67	0.116	0.554

**APPENDIX IV: DATA FOR FREE-FLOW ARMTEC OVERSHOT GATE WITH SIDE CONTRACTIONS**

Test series #4

Test date: October 14, 1993

Gate angle: 36.4°

Contraction ratio: 0.84

Run #	Head (mm)	Discharge (l/s)	Head (ft)	Discharge (cfs)
14	89.9	58.35	0.295	2.061
15	98.1	66.83	0.322	2.360
16	105.8	75.04	0.347	2.650
17	117.7	87.95	0.386	3.106
18	128.0	100.19	0.420	3.538
19	82.6	51.46	0.271	1.817
20	73.5	43.15	0.241	1.524
21	65.8	36.40	0.216	1.286
22	58.2	30.29	0.191	1.070
23	52.4	25.80	0.172	0.911
24	98.5	67.23	0.323	2.374
25	128.6	100.86	0.422	3.562

Test series #4

Test date: October 29, 1993

Gate angle: 36.4°

Contraction ratio: 0.57

Run #	Head (mm)	Discharge (l/s)	Head (ft)	Discharge (cfs)
28	109.4	54.88	0.359	1.938
29	123.7	66.36	0.406	2.344
30	136.9	77.63	0.449	2.741
31	150.9	89.78	0.495	3.171
32	162.5	100.08	0.533	3.534
33	93.9	43.77	0.308	1.546
34	83.8	36.89	0.275	1.303
35	68.9	27.52	0.226	0.972
36	58.5	21.51	0.192	0.760
37	112.8	57.64	0.370	2.035

Test series #7

Test date: September 24, 1993

Gate angle: 54.2°

Contraction ratio: 0.84

Run #	Head (mm)	Discharge (l/s)	Head (ft)	Discharge (cfs)
16	86.3	54.51	0.283	1.925
17	94.8	62.73	0.311	2.215
18	102.4	70.20	0.336	2.479
19	113.4	82.27	0.372	2.905
20	74.7	43.63	0.245	1.541
21	68.9	38.46	0.226	1.358
22	61.0	32.34	0.200	1.142
23	57.3	29.31	0.188	1.035
24	52.7	26.15	0.173	0.923
25	79.6	47.90	0.261	1.692
26	54.6	27.54	0.179	0.973

Test series #7

Test date: October 6, 1993

Gate angle: 54.2°

Contraction ratio: 0.51

Run #	Head (mm)	Discharge (l/s)	Head (ft)	Discharge (cfs)
27	109.4	47.18	0.359	1.666
28	105.2	44.36	0.345	1.567
29	97.8	40.06	0.321	1.415
30	89.6	34.85	0.294	1.231
31	80.8	30.06	0.265	1.062
32	73.8	26.11	0.242	0.922
33	66.1	22.32	0.217	0.788
34	57.6	18.11	0.189	0.640
35	99.1	40.36	0.325	1.425
36	77.4	28.21	0.254	0.996

Test series #8

Test date: December 8, 1993

Gate angle: 63.4°

Contraction ratio: 0.84

Run #	Head (mm)	Discharge (l/s)	Head (ft)	Discharge (cfs)
1	72.8	42.73	0.239	1.509
2	87.5	55.81	0.287	1.971
3	64.9	36.00	0.213	1.271
4	56.1	29.09	0.184	1.027
5	50.0	24.85	0.164	0.878
6	44.5	20.85	0.146	0.736
7	37.5	16.45	0.123	0.581

**APPENDIX V. DATA FOR SUBMERGED ARMTEC OVERSHOT GATE**

Test series #2

Submergence test #1

Test date: July 14, 1993

Gate angle: 28.6°

Free-overfall head: 81.4 mm (0.267 ft)

Discharge: 54.93 l/s (1.940 cfs)

Upstream Head (mm)	Downstream Head (mm)	Upstream Head (ft)	Downstream Head (ft)
81.7	14.9	0.268	0.049
82.0	16.2	0.269	0.053
82.0	18.3	0.269	0.060
82.6	20.4	0.271	0.067
82.9	22.9	0.272	0.075
83.5	27.1	0.274	0.089
84.4	32.0	0.277	0.105
85.3	38.7	0.280	0.127
87.2	46.3	0.286	0.152
89.0	52.7	0.292	0.173
91.1	59.7	0.299	0.196
93.9	66.8	0.308	0.219
96.9	73.8	0.318	0.242
100.6	82.0	0.330	0.269
105.8	90.2	0.347	0.296
114.0	101.5	0.374	0.333
119.5	108.5	0.392	0.356
125.9	116.4	0.413	0.382
132.9	125.3	0.436	0.411
141.1	134.1	0.463	0.440
150.6	145.1	0.494	0.476
160.0	155.8	0.525	0.511

Test series #2

Submergence test #2

Test date: July 15, 1993

Gate angle: 28.6°

Free-overfall head: 61.3 mm (0.201 ft)

Discharge: 35.25 l/s (1.245 cfs)

Upstream Head (mm)	Downstream Head (mm)	Upstream Head (ft)	Downstream Head (ft)
61.6	10.7	0.202	0.035
61.9	11.3	0.203	0.037
62.2	13.4	0.204	0.044
62.8	18.3	0.206	0.060
63.4	22.6	0.208	0.074
64.3	27.4	0.211	0.090
67.7	41.1	0.222	0.135
69.2	45.4	0.227	0.149
70.7	49.7	0.232	0.163
72.8	53.9	0.239	0.177
75.0	58.5	0.246	0.192
77.7	62.8	0.255	0.206
80.2	67.4	0.263	0.221
83.2	71.6	0.273	0.235
86.6	76.2	0.284	0.250
89.3	80.8	0.293	0.265
93.3	85.3	0.306	0.280
97.2	89.3	0.319	0.293
100.9	94.5	0.331	0.310
105.2	98.5	0.345	0.323

Test series #2

Submergence test #3

Test date: July 16, 1993

Gate angle: 28.6°

Free-overfall head: 114.6 mm (0.376 ft)

Discharge: 91.97 l/s (3.248 cfs)

Upstream Head (mm)	Downstream Head (mm)	Upstream Head (ft)	Downstream Head (ft)
115.2	28.0	0.378	0.092
115.8	30.8	0.380	0.101
116.1	35.7	0.381	0.117
117.0	39.9	0.384	0.131
117.7	44.5	0.386	0.146
118.3	49.1	0.388	0.161
119.8	56.1	0.393	0.184
121.3	63.1	0.398	0.207
123.1	70.1	0.404	0.230
125.3	76.8	0.411	0.252
127.1	83.8	0.417	0.275
129.5	90.5	0.425	0.297
132.6	97.5	0.435	0.320
135.3	103.9	0.444	0.341
138.1	110.3	0.453	0.362
142.0	117.0	0.466	0.384
146.0	123.7	0.479	0.406
150.6	130.8	0.494	0.429
155.1	136.6	0.509	0.448
160.3	144.2	0.526	0.473
165.8	150.6	0.544	0.494
171.3	157.9	0.562	0.518
176.2	164.6	0.578	0.540
182.3	171.3	0.598	0.562
188.1	177.7	0.617	0.583
194.2	184.7	0.637	0.606

Test series #2

Submergence test #4

Test date: July 19, 1993

Gate angle: 28.6°

Free-overfall head: 98.5 mm (0.323 ft)

Discharge: 73.03 l/s (2.579 cfs)

Upstream Head (mm)	Downstream Head (mm)	Upstream Head (ft)	Downstream Head (ft)
99.1	17.7	0.325	0.058
99.4	19.2	0.326	0.063
99.7	24.4	0.327	0.080
100.3	29.0	0.329	0.095
100.9	33.5	0.331	0.110
102.1	40.2	0.335	0.132
103.3	47.9	0.339	0.157
105.2	54.3	0.345	0.178
106.7	62.5	0.350	0.205
108.5	68.6	0.356	0.225
110.6	75.0	0.363	0.246
113.4	81.4	0.372	0.267
116.7	88.4	0.383	0.290
120.1	94.8	0.394	0.311
123.4	101.5	0.405	0.333
127.7	107.9	0.419	0.354
131.7	114.6	0.432	0.376
136.9	120.1	0.449	0.394
141.7	128.3	0.465	0.421
146.9	134.4	0.482	0.441
152.1	142.0	0.499	0.466
159.7	149.7	0.524	0.491
165.8	156.7	0.544	0.514
171.6	161.8	0.563	0.531
177.7	168.2	0.583	0.552
183.8	173.1	0.603	0.568

**Test series #3****Submergence test #1**

Test date: July 22, 1993

Gate angle: 22.4°

Free-overfall head: 157.6 mm (0.517 ft)

Discharge: 149.6 l/s (5.282 cfs)

Upstream Head (mm)	Downstream Head (mm)	Upstream Head (ft)	Downstream Head (ft)
158.2	49.1	0.519	0.161
158.2	50.6	0.519	0.166
158.8	56.4	0.521	0.185
159.1	61.6	0.522	0.202
160.3	67.7	0.526	0.222
161.2	74.1	0.529	0.243
162.5	80.8	0.533	0.265
163.7	88.1	0.537	0.289
165.2	95.1	0.542	0.312
166.4	101.8	0.546	0.334
168.6	108.5	0.553	0.356
171.3	118.6	0.562	0.389
174.3	127.4	0.572	0.418
178.0	137.2	0.584	0.450
182.6	147.8	0.599	0.485
186.2	153.3	0.611	0.503
189.3	160.3	0.621	0.526
193.5	167.3	0.635	0.549
197.8	174.3	0.649	0.572
204.2	183.2	0.670	0.601
211.2	192.6	0.693	0.632
217.3	202.1	0.713	0.663
226.5	211.5	0.743	0.694
232.9	221.6	0.764	0.727
242.3	230.4	0.795	0.756

**Test series #3****Submergence test #3**

Test date: July 23, 1993

Gate angle: 22.4°

Free-overfall head: 70.7 mm (0.232 ft)

Discharge: 42.99 l/s (1.518 cfs)

Upstream Head (mm)	Downstream Head (mm)	Upstream Head (ft)	Downstream Head (ft)
71.0	9.4	0.233	0.031
71.3	14.0	0.234	0.046
72.2	20.7	0.237	0.068
73.2	27.4	0.240	0.090
74.1	34.7	0.243	0.114
75.6	41.5	0.248	0.136
77.1	48.8	0.253	0.160
79.6	55.5	0.261	0.182
82.3	62.5	0.270	0.205
85.6	69.2	0.281	0.227
89.9	76.2	0.295	0.250
94.2	82.9	0.309	0.272
99.4	90.2	0.326	0.296
105.2	96.9	0.345	0.318
110.9	103.9	0.364	0.341
117.0	110.3	0.384	0.362
123.1	117.3	0.404	0.385

**Test series #3****Submergence test #2**

Test date: July 23, 1993

Gate angle: 22.4°

Free-overfall head: 87.2 mm (0.286 ft)

Discharge: 58.98 l/s (2.083 cfs)

Upstream Head (mm)	Downstream Head (mm)	Upstream Head (ft)	Downstream Head (ft)
87.8	21.9	0.288	0.072
88.4	26.5	0.290	0.087
89.0	31.1	0.292	0.102
89.9	38.1	0.295	0.125
91.1	45.1	0.299	0.148
92.7	52.1	0.304	0.171
94.2	58.8	0.309	0.193
96.0	65.5	0.315	0.215
98.8	72.5	0.324	0.238
101.8	78.9	0.334	0.259
105.5	86.0	0.346	0.282
109.1	93.0	0.358	0.305
114.0	100.3	0.374	0.329
118.6	107.0	0.389	0.351
124.1	113.4	0.407	0.372
129.8	120.1	0.426	0.394
135.6	127.1	0.445	0.417
143.3	135.6	0.470	0.445

**Test series #3****Submergence test #4**

Test date: July 26, 1993

Gate angle: 22.4°

Free-overfall head: 103.3 mm (0.339 ft)

Discharge: 77.02 l/s (2.720 cfs)

Upstream Head (mm)	Downstream Head (mm)	Upstream Head (ft)	Downstream Head (ft)
103.9	25.0	0.341	0.082
104.2	29.9	0.342	0.098
105.2	37.2	0.345	0.122
106.1	44.2	0.348	0.145
107.3	51.8	0.352	0.170
108.5	58.2	0.356	0.191
110.0	64.9	0.361	0.213
111.6	71.9	0.366	0.236
114.0	78.9	0.374	0.259
116.4	86.0	0.382	0.282
119.2	93.0	0.391	0.305
122.8	100.0	0.403	0.328
127.1	107.0	0.417	0.351
131.1	113.4	0.430	0.372
137.8	123.1	0.452	0.404
144.8	131.7	0.475	0.432
152.4	141.1	0.500	0.463
159.4	149.4	0.523	0.490
167.3	157.6	0.549	0.517
175.3	168.2	0.575	0.552

Test series #3  
 Submergence test #5  
 Test date: July 26, 1993  
 Gate angle: 22.4°  
 Free-overfall head: 123.7 mm (0.406 ft)  
 Discharge: 102.1 l/s (3.605 cfs)

Upstream Head (mm)	Downstream Head (mm)	Upstream Head (ft)	Downstream Head (ft)
124.4	39.6	0.408	0.130
125.0	42.1	0.410	0.138
125.9	47.9	0.413	0.157
126.8	56.1	0.416	0.184
128.3	62.8	0.421	0.206
129.2	69.5	0.424	0.228
131.1	73.8	0.430	0.242
133.8	82.9	0.439	0.272
141.4	110.3	0.464	0.362
146.3	122.2	0.480	0.401
151.8	128.9	0.498	0.423
158.2	137.8	0.519	0.452
164.6	147.8	0.540	0.485
171.3	157.3	0.562	0.516
178.3	166.7	0.585	0.547
185.6	175.6	0.609	0.576
193.9	184.1	0.636	0.604

Test series #3  
 Submergence test #6  
 Test date: July 27, 1993  
 Gate angle: 22.4°  
 Free-overfall head: 141.4 mm (0.464 ft)  
 Discharge: 125.7 l/s (4.440 cfs)

Upstream Head (mm)	Downstream Head (mm)	Upstream Head (ft)	Downstream Head (ft)
142.0	43.0	0.466	0.141
142.6	48.2	0.468	0.158
143.6	55.5	0.471	0.182
144.5	62.8	0.474	0.206
145.7	69.5	0.478	0.228
146.9	77.7	0.482	0.255
148.4	84.1	0.487	0.276
149.7	91.7	0.491	0.301
151.8	97.2	0.498	0.319
153.3	105.2	0.503	0.345
155.4	111.9	0.510	0.367
159.1	121.9	0.522	0.400
163.4	131.1	0.536	0.430
168.6	141.1	0.553	0.463
175.0	151.2	0.574	0.496
179.8	160.0	0.590	0.525
185.3	167.3	0.608	0.549
210.6	199.0	0.691	0.653
215.8	205.7	0.708	0.675

Test series #3  
 Submergence test #7  
 Test date: July 27, 1993  
 Gate angle: 22.4°  
 Free-overfall head: 159.1 mm (0.522 ft)  
 Discharge: 151.7 l/s (5.358 cfs)

Upstream Head (mm)	Downstream Head (mm)	Upstream Head (ft)	Downstream Head (ft)
159.7	49.4	0.524	0.162
160.3	54.9	0.526	0.180
160.9	62.5	0.528	0.205
162.2	69.2	0.532	0.227
162.8	76.2	0.534	0.250
164.6	83.2	0.540	0.273
165.2	90.2	0.542	0.296
166.7	96.9	0.547	0.318
168.2	104.2	0.552	0.342
170.7	114.0	0.560	0.374
173.1	122.8	0.568	0.403
176.2	132.3	0.578	0.434
179.8	139.3	0.590	0.457
184.4	149.0	0.605	0.489
189.0	158.5	0.620	0.520
193.9	167.0	0.636	0.548
199.9	176.2	0.656	0.578
205.7	185.6	0.675	0.609
212.8	194.2	0.698	0.637
220.1	204.2	0.722	0.670
227.7	213.4	0.747	0.700
235.9	221.0	0.774	0.725

Test series #4  
 Submergence test #1  
 Test date: July 30, 1993  
 Gate angle: 36.4°  
 Free-overfall head: 84.1 mm (0.276 ft)  
 Discharge: 57.26 l/s (2.022 cfs)

Upstream Head (mm)	Downstream Head (mm)	Upstream Head (ft)	Downstream Head (ft)
84.7	12.8	0.278	0.042
85.3	17.7	0.280	0.058
86.3	24.4	0.283	0.080
87.5	31.1	0.287	0.102
88.7	37.8	0.291	0.124
90.2	44.2	0.296	0.145
92.0	51.2	0.302	0.168
93.9	57.6	0.308	0.189
96.6	64.6	0.317	0.212
99.1	71.3	0.325	0.234
102.4	77.7	0.336	0.255
106.1	84.1	0.348	0.276
110.0	91.1	0.361	0.299
114.6	97.5	0.376	0.320
118.6	103.9	0.389	0.341
123.4	110.6	0.405	0.363
128.3	117.7	0.421	0.386
135.9	126.2	0.446	0.414
146.0	137.8	0.479	0.452
154.8	147.2	0.508	0.483
163.1	156.7	0.535	0.514

Test series #4

Submergence test #2  
 Test date: July 30, 1993  
 Gate angle: 36.4°  
 Free-overfall head: 61.0 mm (0.200 ft)  
 Discharge: 35.28 l/s (1.246 cfs)

Upstream Head (mm)	Downstream Head (mm)	Upstream Head (ft)	Downstream Head (ft)
61.6	7.32	0.202	0.024
62.5	14.0	0.205	0.046
63.7	21.0	0.209	0.069
64.9	27.7	0.213	0.091
66.4	34.1	0.218	0.112
68.6	40.8	0.225	0.134
70.7	47.2	0.232	0.155
73.8	54.3	0.242	0.178
77.4	60.7	0.254	0.199
81.4	67.7	0.267	0.222
85.6	74.1	0.281	0.243
90.5	80.8	0.297	0.265
96.0	87.2	0.315	0.286
101.2	93.6	0.332	0.307
107.0	100.6	0.351	0.330
113.1	107.0	0.371	0.351

Test series #4

Submergence test #3  
 Test date: August 2, 1993  
 Gate angle: 36.4°  
 Free-overfall head: 101.5 mm (0.333 ft)  
 Discharge: 76.09 l/s (2.687 cfs)

Upstream Head (mm)	Downstream Head (mm)	Upstream Head (ft)	Downstream Head (ft)
102.1	18.0	0.335	0.059
103.0	24.4	0.338	0.080
103.9	31.7	0.341	0.104
105.2	38.4	0.345	0.126
106.4	45.4	0.349	0.149
107.9	52.1	0.354	0.171
109.7	59.1	0.360	0.194
111.6	65.2	0.366	0.214
113.4	71.6	0.372	0.235
115.8	78.6	0.380	0.258
118.6	85.3	0.389	0.280
121.6	92.0	0.399	0.302
125.3	99.1	0.411	0.325
128.3	105.5	0.421	0.346
132.6	112.2	0.435	0.368
136.9	118.9	0.449	0.390
141.7	125.3	0.465	0.411
146.9	131.7	0.482	0.432
153.6	140.8	0.504	0.462
160.6	149.0	0.527	0.489
167.9	157.9	0.551	0.518
175.9	166.4	0.577	0.546
183.5	175.6	0.602	0.576

Test series #4

Submergence test #4  
 Test date: August 2, 1993  
 Gate angle: 36.4°  
 Free-overfall head: 69.2 mm (0.227 ft)  
 Discharge: 42.59 l/s (1.504 cfs)

Upstream Head (mm)	Downstream Head (mm)	Upstream Head (ft)	Downstream Head (ft)
69.8	9.14	0.229	0.030
70.7	16.2	0.232	0.053
71.6	22.9	0.235	0.075
72.8	29.9	0.239	0.098
74.4	36.0	0.244	0.118
76.2	42.7	0.250	0.140
78.3	49.7	0.257	0.163
80.8	56.1	0.265	0.184
83.8	63.1	0.275	0.207
87.5	69.8	0.287	0.229
91.7	76.5	0.301	0.251
96.0	82.9	0.315	0.272
101.2	89.6	0.332	0.294
107.6	98.1	0.353	0.322
115.5	107.3	0.379	0.352
122.5	115.8	0.402	0.380
130.8	124.7	0.429	0.409

Test series #5

Submergence test #1  
 Test date: August 5, 1993  
 Gate angle: 16.2°  
 Free-overfall head: 118.3 mm (0.388 ft)  
 Discharge: 95.27 l/s (3.365 cfs)

Upstream Head (mm)	Downstream Head (mm)	Upstream Head (ft)	Downstream Head (ft)
118.9	35.4	0.390	0.116
119.2	41.1	0.391	0.135
120.1	49.4	0.394	0.162
120.7	56.7	0.396	0.186
122.2	62.8	0.401	0.206
122.8	70.1	0.403	0.230
123.1	72.2	0.404	0.237
124.7	79.2	0.409	0.260
126.5	86.0	0.415	0.282
128.3	93.6	0.421	0.307
135.6	112.2	0.445	0.368
139.3	119.2	0.457	0.391
143.9	126.2	0.472	0.414
148.7	133.8	0.488	0.439
153.6	140.8	0.504	0.462
159.4	147.8	0.523	0.485
165.5	155.1	0.543	0.509
171.0	161.8	0.561	0.531
178.9	171.3	0.587	0.562
189.9	185.0	0.623	0.607

Test series #5  
 Submergence test #2  
 Test date: August 6, 1993  
 Gate angle: 16.2°  
 Free-overfall head: 150.3 mm (0.493 ft)  
 Discharge: 139.0 Vs (4.908 cfs)

Upstream Head (mm)	Downstream Head (mm)	Upstream Head (ft)	Downstream Head (ft)
150.6	49.1	0.494	0.161
150.9	55.8	0.495	0.183
152.1	64.9	0.499	0.213
153.0	74.1	0.502	0.243
154.5	85.0	0.507	0.279
156.4	94.5	0.513	0.310
157.9	103.0	0.518	0.338
159.7	110.6	0.524	0.363
162.5	120.4	0.533	0.395
165.5	129.5	0.543	0.425
169.5	129.5	0.556	0.425
174.0	147.8	0.571	0.485
179.2	157.0	0.588	0.515
185.6	166.1	0.609	0.545
191.7	175.0	0.629	0.574
198.4	183.8	0.651	0.603
205.7	193.2	0.675	0.634
213.7	202.1	0.701	0.663
221.6	211.2	0.727	0.693

Test series #5  
 Submergence test #5  
 Test date: August 11, 1993  
 Gate angle: 16.2°  
 Free-overfall head: 97.2 mm (0.319 ft)  
 Discharge: 68.70 Vs (2.426 cfs)

Upstream Head (mm)	Downstream Head (mm)	Upstream Head (ft)	Downstream Head (ft)
97.5	21.0	0.320	0.069
97.8	28.3	0.321	0.093
98.5	36.0	0.323	0.118
99.1	43.3	0.325	0.142
100.6	50.0	0.330	0.164
101.5	57.0	0.333	0.187
103.0	65.5	0.338	0.215
104.5	71.3	0.343	0.234
106.7	79.2	0.350	0.260
109.4	86.0	0.359	0.282
112.8	93.6	0.370	0.307
116.7	99.4	0.383	0.326
121.0	106.7	0.397	0.350
125.9	114.0	0.413	0.374
131.4	121.0	0.431	0.397
136.9	128.3	0.449	0.421
142.6	134.7	0.468	0.442

Test series #5  
 Submergence test #4  
 Test date: August 11, 1993  
 Gate angle: 16.2°  
 Free-overfall head: 71.9 mm (0.236 ft)  
 Discharge: 42.25 Vs (1.492 cfs)

Upstream Head (mm)	Downstream Head (mm)	Upstream Head (ft)	Downstream Head (ft)
72.5	15.2	0.238	0.050
72.8	22.3	0.239	0.073
73.8	29.9	0.242	0.098
74.7	36.9	0.245	0.121
75.9	43.9	0.249	0.144
77.4	50.6	0.254	0.166
79.6	58.2	0.261	0.191
82.3	64.9	0.270	0.213
86.0	71.9	0.282	0.236
90.2	78.9	0.296	0.259
95.1	85.6	0.312	0.281
100.6	92.4	0.330	0.303
106.1	99.7	0.348	0.327
114.3	109.1	0.375	0.358

Test series #6  
 Submergence test #1  
 Test date: August 23, 1993  
 Gate angle: 43.6°  
 Free-overfall head: 98.8 mm (0.324 ft)  
 Discharge: 73.23 Vs (2.586 cfs)

Upstream Head (mm)	Downstream Head (mm)	Upstream Head (ft)	Downstream Head (ft)
99.4	15.2	0.326	0.050
100.3	21.9	0.329	0.072
101.2	28.7	0.332	0.094
102.7	35.7	0.337	0.117
103.9	42.4	0.341	0.139
105.5	48.8	0.346	0.160
107.0	55.5	0.351	0.182
109.1	60.7	0.358	0.199
111.3	67.7	0.365	0.222
113.7	74.4	0.373	0.244
116.4	82.0	0.382	0.269
119.8	88.4	0.393	0.290
124.7	98.1	0.409	0.322
130.8	108.5	0.429	0.356
147.2	130.1	0.483	0.427
155.8	143.9	0.511	0.472
166.1	154.8	0.545	0.508

**Test series #6**

**Submergence test #2**

Test date: August 23, 1993

Gate angle: 43.6°

Free-overfall head: 78.9 mm (0.259 ft)

Discharge: 52.02 l/s (1.837 cfs)

Upstream Head (mm)	Downstream Head (mm)	Upstream Head (ft)	Downstream Head (ft)
79.2	8.84	0.260	0.029
80.2	16.2	0.263	0.053
81.4	22.6	0.267	0.074
82.0	29.6	0.269	0.097
83.8	36.3	0.275	0.119
85.6	42.1	0.281	0.138
87.5	45.7	0.287	0.150
89.6	55.5	0.294	0.182
92.4	61.9	0.303	0.203
95.1	68.9	0.312	0.226
98.5	75.0	0.323	0.246
102.1	81.7	0.335	0.268
106.1	88.1	0.348	0.289
110.3	94.8	0.362	0.311
115.2	101.5	0.378	0.333
120.1	108.2	0.394	0.355
125.9	115.2	0.413	0.378
131.7	122.5	0.432	0.402

**Test series #6**

**Submergence test #4**

Test date: August 24, 1993

Gate angle: 43.6°

Free-overfall head: 112.2 mm (0.368 ft)

Discharge: 89.20 l/s (3.150 cfs)

Upstream Head (mm)	Downstream Head (mm)	Upstream Head (ft)	Downstream Head (ft)
112.8	19.5	0.370	0.064
114.0	26.2	0.374	0.086
114.9	33.2	0.377	0.109
116.4	39.9	0.382	0.131
117.3	46.6	0.385	0.153
118.9	53.6	0.390	0.176
120.7	60.7	0.396	0.199
122.5	67.4	0.402	0.221
124.7	71.9	0.409	0.236
127.1	79.6	0.417	0.261
129.5	87.2	0.425	0.286
132.0	96.9	0.433	0.318
135.3	100.6	0.444	0.330
138.4	107.6	0.454	0.353
142.0	114.0	0.466	0.374
146.0	120.4	0.479	0.395
150.3	127.1	0.493	0.417
154.8	133.8	0.508	0.439
159.7	140.8	0.524	0.462
164.3	147.5	0.539	0.484
170.1	154.5	0.558	0.507
176.2	161.8	0.578	0.531

**Test series #6**

**Submergence test #5**

Test date: August 25, 1993

Gate angle: 43.6°

Free-overfall head: 69.2 mm (0.227 ft)

Discharge: 42.99 l/s (1.518 cfs)

Upstream Head (mm)	Downstream Head (mm)	Upstream Head (ft)	Downstream Head (ft)
69.5	5.18	0.228	0.017
70.1	11.9	0.230	0.039
71.3	18.3	0.234	0.060
72.8	25.6	0.239	0.084
74.1	31.4	0.243	0.103
75.6	38.4	0.248	0.126
77.7	45.4	0.255	0.149
81.1	53.6	0.266	0.176
84.1	60.7	0.276	0.199
87.5	67.4	0.287	0.221
91.1	73.8	0.299	0.242
95.1	80.2	0.312	0.263
99.7	86.3	0.327	0.283
104.9	93.0	0.344	0.305
110.0	99.7	0.361	0.327
115.5	106.4	0.379	0.349
121.3	113.4	0.398	0.372
127.7	120.4	0.419	0.395

**Test series #6**

**Submergence test #6**

Test date: August 25, 1993

Gate angle: 43.6°

Free-overfall head: 60.7 mm (0.199 ft)

Discharge: 34.83 l/s (1.230 cfs)

Upstream Head (mm)	Downstream Head (mm)	Upstream Head (ft)	Downstream Head (ft)
61.5	0.26	0.202	0.001
61.5	7.26	0.202	0.024
62.4	14.0	0.205	0.046
63.6	21.0	0.209	0.069
65.1	27.4	0.214	0.090
66.9	34.4	0.220	0.113
68.8	40.8	0.226	0.134
71.2	47.8	0.234	0.157
74.6	54.2	0.245	0.178
77.9	60.5	0.256	0.199
81.6	66.6	0.268	0.219
85.8	73.0	0.282	0.240
90.4	79.7	0.297	0.262
95.6	86.4	0.314	0.284
101.1	92.8	0.332	0.305
106.5	99.8	0.350	0.328
112.6	106.5	0.370	0.350

Test series #6

Submergence test #8

Test date: August 26, 1993

Gate angle: 43.6°

Free-overfall head: 51.5 mm (0.169 ft)

Discharge: 27.16 l/s (0.959 cfs)

Upstream Head (mm)	Downstream Head (mm)	Upstream Head (ft)	Downstream Head (ft)
51.8	4.27	0.170	0.014
52.7	10.4	0.173	0.034
53.9	17.1	0.177	0.056
55.2	24.1	0.181	0.079
57.6	31.1	0.189	0.102
59.4	37.2	0.195	0.122
62.2	43.6	0.204	0.143
65.8	50.3	0.216	0.165
69.5	56.7	0.228	0.186
73.5	63.1	0.241	0.207
78.6	70.1	0.258	0.230
83.5	76.5	0.274	0.251
88.7	82.3	0.291	0.270
94.2	89.0	0.309	0.292

Test series #7

Submergence test #1

Test date: September 9, 1993

Gate angle: 54.2°

Free-overfall head: 60.0 mm (0.197 ft)

Discharge: 34.21 l/s (1.208 cfs)

Upstream Head (mm)	Downstream Head (mm)	Upstream Head (ft)	Downstream Head (ft)
60.4	3.35	0.198	0.011
61.6	10.4	0.202	0.034
63.1	16.5	0.207	0.054
64.6	22.3	0.212	0.073
65.8	29.0	0.216	0.095
68.0	35.4	0.223	0.116
70.1	42.1	0.230	0.138
72.8	48.5	0.239	0.159
75.9	55.5	0.249	0.182
79.9	62.2	0.262	0.204
84.4	70.1	0.277	0.230
91.7	79.6	0.301	0.261
99.1	89.9	0.325	0.295
105.8	97.5	0.347	0.320
112.8	106.1	0.370	0.348
119.8	113.4	0.393	0.372
126.5	121.3	0.415	0.398

Test series #7

Submergence test #3

Test date: September 15, 1993

Gate angle: 54.2°

Free-overfall head: 69.8 mm (0.229 ft)

Discharge: 42.96 l/s (1.517 cfs)

Upstream Head (mm)	Downstream Head (mm)	Upstream Head (ft)	Downstream Head (ft)
70.1	4.88	0.230	0.016
71.0	11.6	0.233	0.038
71.9	18.3	0.236	0.060
73.5	25.0	0.241	0.082
75.0	30.8	0.246	0.101
76.8	36.9	0.252	0.121
78.9	43.3	0.259	0.142
81.1	49.7	0.266	0.163
83.8	56.4	0.275	0.185
86.6	62.5	0.284	0.205
90.2	68.9	0.296	0.226
93.9	75.6	0.308	0.248
98.1	82.0	0.322	0.269
103.0	89.6	0.338	0.294
108.5	96.9	0.356	0.318
114.0	103.6	0.374	0.340
119.2	110.0	0.391	0.361

Test series #7

Submergence test #4

Test date: September 17, 1993

Gate angle: 54.2°

Free-overfall head: 44.2 mm (0.145 ft)

Discharge: 21.44 l/s (0.757 cfs)

Upstream Head (mm)	Downstream Head (mm)	Upstream Head (ft)	Downstream Head (ft)
44.8	4.57	0.147	0.015
46.0	11.0	0.151	0.036
47.2	17.4	0.155	0.057
49.1	23.8	0.161	0.078
50.9	29.6	0.167	0.097
53.6	36.3	0.176	0.119
56.7	42.7	0.186	0.140
60.0	48.5	0.197	0.159
64.0	54.9	0.210	0.180
68.9	61.0	0.226	0.200
74.1	67.4	0.243	0.221
79.2	73.8	0.260	0.242
85.0	80.2	0.279	0.263
90.8	86.6	0.298	0.284

**APPENDIX VI. DATA FOR SUBMERGED ARMTEC OVERSHOT GATE WITH SIDE CONTRACTIONS**

Test series #4  
 Submergence test #5  
 Contraction ratio: 0.84  
 Test date: October 20, 1993  
 Gate angle: 36.4°  
 Free-overfall head: 98.5 mm (0.323 ft)  
 Discharge: 67.22 Vs (2.374 cfs)

Upstream Head (mm)	Downstream Head (mm)	Upstream Head (ft)	Downstream Head (ft)
99.1	17.4	0.325	0.057
100.0	25.6	0.328	0.084
101.2	31.7	0.332	0.104
102.4	38.7	0.336	0.127
103.9	45.7	0.341	0.150
105.5	52.7	0.346	0.173
107.3	61.3	0.352	0.201
109.1	67.1	0.358	0.220
111.6	73.8	0.366	0.242
114.3	81.1	0.375	0.266
117.7	88.1	0.386	0.289
121.0	94.8	0.397	0.311
124.7	101.2	0.409	0.332
128.6	107.9	0.422	0.354
133.2	114.6	0.437	0.376
137.5	121.3	0.451	0.398
142.3	127.7	0.467	0.419
147.5	134.4	0.484	0.441
153.0	140.8	0.502	0.462

Test series #4  
 Submergence test #6  
 Contraction ratio: 0.84  
 Test date: October 21, 1993  
 Gate angle: 36.4°  
 Free-overfall head: 128.6 mm (0.422 ft)  
 Discharge: 100.9 Vs (3.562 cfs)

Upstream Head (mm)	Downstream Head (mm)	Upstream Head (ft)	Downstream Head (ft)
128.9	23.8	0.423	0.078
129.8	31.7	0.426	0.104
131.4	42.4	0.431	0.139
132.3	47.5	0.434	0.156
133.5	54.6	0.438	0.179
135.0	61.6	0.443	0.202
136.6	68.9	0.448	0.226
138.4	75.9	0.454	0.249
140.2	80.5	0.460	0.264
142.3	88.4	0.467	0.290
144.8	96.0	0.475	0.315
147.2	103.9	0.483	0.341
150.3	110.3	0.493	0.362
153.3	117.7	0.503	0.386
156.7	124.1	0.514	0.407
161.5	133.2	0.530	0.437
167.0	142.3	0.548	0.467
172.8	151.5	0.567	0.497
179.5	160.3	0.589	0.526
186.2	169.5	0.611	0.556

Test series #4  
 Submergence test #7  
 Contraction ratio: 0.84  
 Test date: October 25, 1993  
 Gate angle: 36.4°  
 Free-overfall head: 73.2 mm (0.240 ft)  
 Discharge: 42.90 Vs (1.515 cfs)

Upstream Head (mm)	Downstream Head (mm)	Upstream Head (ft)	Downstream Head (ft)
73.5	7.32	0.241	0.024
73.8	10.1	0.242	0.033
74.1	12.2	0.243	0.040
75.0	19.2	0.246	0.063
76.5	26.5	0.251	0.087
77.7	33.8	0.255	0.111
79.6	40.2	0.261	0.132
81.4	47.9	0.267	0.157
83.5	53.9	0.274	0.177
86.0	60.7	0.282	0.199
89.0	67.4	0.292	0.221
92.7	74.1	0.304	0.243
96.6	80.8	0.317	0.265
101.2	87.2	0.332	0.286
105.8	93.9	0.347	0.308
110.9	100.3	0.364	0.329
116.4	107.0	0.382	0.351

Test series #4  
 Submergence test #8  
 Contraction ratio: 0.84  
 Test date: October 26, 1993  
 Gate angle: 36.4°  
 Free-overfall head: 50.9 mm (0.167 ft)  
 Discharge: 24.89 Vs (0.879 cfs)

Upstream Head (mm)	Downstream Head (mm)	Upstream Head (ft)	Downstream Head (ft)
51.2	2.13	0.168	0.007
51.5	4.57	0.169	0.015
52.4	9.14	0.172	0.030
53.3	15.5	0.175	0.051
54.9	22.6	0.180	0.074
56.4	29.3	0.185	0.096
58.5	36.0	0.192	0.118
61.3	43.0	0.201	0.141
64.6	49.4	0.212	0.162
68.3	55.8	0.224	0.183
72.5	62.2	0.238	0.204
77.1	68.9	0.253	0.226
82.6	75.3	0.271	0.247
88.1	82.0	0.289	0.269

Test series #4

Submergence test #9

Contraction ratio: 0.59

Test date: November 1, 1993

Gate angle: 36.4°

Free-overfall head: 112.8 mm (0.370 ft)

Discharge: 57.62 Vs (2.035 cfs)

Upstream Head (mm)	Downstream Head (mm)	Upstream Head (ft)	Downstream Head (ft)
113.1	13.1	0.371	0.043
113.1	14.3	0.371	0.047
113.4	16.8	0.372	0.055
114.0	21.6	0.374	0.071
114.9	28.0	0.377	0.092
116.1	35.1	0.381	0.115
117.3	42.7	0.385	0.140
118.9	49.7	0.390	0.163
120.4	57.0	0.395	0.187
121.9	62.8	0.400	0.206
123.7	70.4	0.406	0.231
126.5	77.4	0.415	0.254
128.3	84.1	0.421	0.276
131.1	90.8	0.430	0.298
134.1	97.8	0.440	0.321
137.5	104.2	0.451	0.342
142.0	113.4	0.466	0.372
147.5	122.2	0.484	0.401
153.6	131.4	0.504	0.431
160.0	140.5	0.525	0.461
166.7	149.4	0.547	0.490
174.0	158.5	0.571	0.520

Test series #7

Submergence test #5

Contraction ratio: 0.84

Test date: September 29, 1993

Gate angle: 54.2°

Free-overfall head: 79.6 mm (0.261 ft)

Discharge: 47.91 Vs (1.692 cfs)

Upstream Head (mm)	Downstream Head (mm)	Upstream Head (ft)	Downstream Head (ft)
79.2	5.2	0.260	0.017
80.2	11.0	0.263	0.036
81.4	17.4	0.267	0.057
82.9	25.3	0.272	0.083
84.1	31.4	0.276	0.103
86.3	36.9	0.283	0.121
87.8	43.6	0.288	0.143
89.9	50.3	0.295	0.165
92.0	56.1	0.302	0.184
94.5	62.8	0.310	0.206
97.5	68.9	0.320	0.226
100.0	75.0	0.328	0.246
103.9	81.7	0.341	0.268
107.9	88.1	0.354	0.289
112.8	95.1	0.370	0.312
117.7	102.7	0.386	0.337
123.4	110.0	0.405	0.361
129.5	117.3	0.425	0.385

Test series #7

Submergence test #6

Contraction ratio: 0.84

Test date: September 30, 1993

Gate angle: 54.2°

Free-overfall head: 54.6 mm (0.179 ft)

Discharge: 27.55 Vs (0.973 cfs)

Upstream Head (mm)	Downstream Head (mm)	Upstream Head (ft)	Downstream Head (ft)
54.9	0.00	0.180	0.000
55.8	5.79	0.183	0.019
56.7	12.5	0.186	0.041
58.2	19.2	0.191	0.063
59.7	26.2	0.196	0.086
61.9	32.0	0.203	0.105
64.0	38.7	0.210	0.127
66.8	45.1	0.219	0.148
69.8	51.5	0.229	0.169
73.5	57.9	0.241	0.190
77.7	64.6	0.255	0.212
82.3	71.0	0.270	0.233
87.5	77.7	0.287	0.255
93.0	84.7	0.305	0.278

Test series #7

Submergence test #7

Contraction ratio: 0.51

Test date: October 8, 1993

Gate angle: 54.2°

Free-overfall head: 99.1 mm (0.325 ft)

Discharge: 40.35 Vs (1.425 cfs)

Upstream Head (mm)	Downstream Head (mm)	Upstream Head (ft)	Downstream Head (ft)
99.7	2.44	0.327	0.008
100.3	9.45	0.329	0.031
100.9	16.2	0.331	0.053
102.1	22.3	0.335	0.073
103.3	28.7	0.339	0.094
104.9	35.1	0.344	0.115
106.4	42.1	0.349	0.138
108.2	48.5	0.355	0.159
110.0	54.6	0.361	0.179
111.9	61.3	0.367	0.201
114.0	67.4	0.374	0.221
116.4	73.5	0.382	0.241
121.0	84.1	0.397	0.276
126.2	94.5	0.414	0.310
130.1	102.1	0.427	0.335

Test series #7

Submergence test #8

Contraction ratio: 0.51

Test date: October 8, 1993

Gate angle: 54.2°

Free-overfall head: 77.4 mm (0.254 ft)

Discharge: 28.20 l/s (0.996 cfs)

Upstream Head (mm)	Downstream Head (mm)	Upstream Head (ft)	Downstream Head (ft)
78.3	6.10	0.257	0.020
79.2	12.5	0.260	0.041
80.5	18.3	0.264	0.060
81.7	25.0	0.268	0.082
83.2	31.7	0.273	0.104
85.0	38.7	0.279	0.127
86.9	44.8	0.285	0.147
89.0	52.1	0.292	0.171
91.4	57.6	0.300	0.189
93.9	63.7	0.308	0.209
98.1	71.6	0.322	0.235
101.8	79.9	0.334	0.262
107.6	88.7	0.353	0.291
113.7	97.5	0.373	0.320

Test series #7

Submergence test #9

Contraction ratio: 0.51

Test date: October 12, 1993

Gate angle: 54.2°

Free-overfall head: 62.2 mm (0.204 ft)

Discharge: 20.05 l/s (0.708 cfs)

Upstream Head (mm)	Downstream Head (mm)	Upstream Head (ft)	Downstream Head (ft)
62.5	2.44	0.205	0.008
63.4	9.14	0.208	0.030
64.6	16.2	0.212	0.053
66.1	22.3	0.217	0.073
67.7	28.7	0.222	0.094
69.5	35.4	0.228	0.116
71.6	41.5	0.235	0.136
74.1	47.5	0.243	0.156
76.8	54.3	0.252	0.178
80.5	60.7	0.264	0.199
83.2	65.8	0.273	0.216
87.2	71.9	0.286	0.236
91.7	78.0	0.301	0.256
96.9	85.3	0.318	0.280

**APPENDIX VII. DATA FOR FREE-FLOW USWCL OVERSHOT GATE**

Test series #7

Test dates: November 5 and 6, 1992

Gate angle: 24.0°

Run #	Head (mm)	Discharge (l/s)	Head (ft)	Discharge (cfs)
1	200.3	238.11	0.657	8.409
2	215.5	266.13	0.707	9.398
3	190.2	219.01	0.624	7.734
4	169.8	182.99	0.557	6.462
5	156.7	161.86	0.514	5.716
6	147.0	146.33	0.482	5.167
7	138.1	133.31	0.453	4.708
8	128.1	117.46	0.420	4.148
9	118.6	105.00	0.389	3.708
10	110.7	93.74	0.363	3.310
11	102.8	82.94	0.337	2.929
12	92.7	70.14	0.304	2.477
13	85.1	61.82	0.279	2.183
14	76.6	52.39	0.251	1.850
15	65.9	41.85	0.216	1.478
16	56.4	32.67	0.185	1.154
17	51.3	28.11	0.168	0.993

Test series #9

Test dates: November 12, 1992

Gate angle: 27.8°

Run #	Head (mm)	Discharge (l/s)	Head (ft)	Discharge (cfs)
1	131.7	122.23	0.432	4.317
2	119.8	107.35	0.393	3.791
3	106.7	89.57	0.350	3.163
4	96.3	75.73	0.316	2.674
5	83.2	60.11	0.273	2.123
6	68.6	44.51	0.225	1.572
7	59.4	35.72	0.195	1.261
8	52.7	29.19	0.173	1.031
9	128.0	122.37	0.420	4.322
10	154.8	159.89	0.508	5.646
11	174.0	189.92	0.571	6.707
12	191.7	221.31	0.629	7.816

Test series #11

Test dates: November 20, 1992

Gate angle: 35.0°

Run #	Head (mm)	Discharge (l/s)	Head (ft)	Discharge (cfs)
1	135.8	130.02	0.445	4.592
2	122.0	111.45	0.400	3.936
3	110.2	94.98	0.361	3.354
4	100.7	83.53	0.330	2.950
5	91.6	71.61	0.300	2.529
6	81.5	59.63	0.267	2.106
7	70.8	47.97	0.232	1.694
8	62.6	39.59	0.205	1.398
9	52.9	31.39	0.173	1.108

Test series #8

Test dates: November 10, 1992

Gate angle: 30.2°

Run #	Head (mm)	Discharge (l/s)	Head (ft)	Discharge (cfs)
1	116.0	101.03	0.380	3.568
2	130.6	121.68	0.428	4.297
3	143.4	140.29	0.470	4.954
4	159.3	164.98	0.522	5.826
5	174.8	190.42	0.573	6.725
6	102.0	83.35	0.334	2.943
7	88.8	67.55	0.291	2.386
8	74.8	51.74	0.245	1.827
9	66.9	42.39	0.219	1.497
10	54.1	31.30	0.177	1.105

Test series #10

Test dates: November 17 and 18, 1992

Gate angle: 25.9°

Run #	Head (mm)	Discharge (l/s)	Head (ft)	Discharge (cfs)
1	148.6	149.70	0.487	5.287
2	165.3	175.41	0.542	6.195
3	175.4	195.87	0.575	6.917
4	190.0	221.01	0.623	7.805
5	138.8	135.89	0.455	4.799
6	129.0	120.35	0.423	4.250
7	119.6	107.65	0.392	3.802
8	107.1	90.79	0.351	3.206
9	94.9	75.39	0.311	2.662
10	84.2	62.98	0.276	2.224
11	78.1	56.21	0.256	1.985
12	67.5	44.79	0.221	1.582
13	59.6	36.74	0.195	1.297
14	53.5	30.92	0.175	1.092

Test series #12

Test dates: November 24 and 25, 1992

Gate angle: 29.8°

Run #	Head (mm)	Discharge (l/s)	Head (ft)	Discharge (cfs)
1	132.1	125.46	0.433	4.431
2	145.2	146.01	0.476	5.156
3	157.4	162.43	0.516	5.736
4	168.3	182.46	0.552	6.444
5	179.6	201.82	0.589	7.127
6	120.2	108.29	0.394	3.824
7	112.9	98.95	0.370	3.494
8	96.7	78.47	0.317	2.771
9	87.9	67.34	0.288	2.378
10	79.3	57.51	0.260	2.031
11	71.4	49.40	0.234	1.745
12	61.7	39.29	0.202	1.388
13	54.0	32.15	0.177	1.135

**APPENDIX VIII. DATA FOR BAZIN'S EXPERIMENTS ON INCLINED WEIRS**

Gate angle: 71.57°

Weir width: 1000 mm (3.281 ft)

Channel width: 1000 mm (3.281 ft)

Crest height above channel bottom: 1133 mm (3.717 ft)

Run #	Head (mm)	Discharge (l/s)	Head (ft)	Discharge (cfs)
14-1	203	181	0.666	6.39
14-2	250	251	0.820	8.86
14-3	299	328	0.981	11.58
14-4	350	414	1.148	14.62
14-5	398	500	1.306	17.66
14-6	447	594	1.467	20.98

Gate angle: 56.31°

Weir width: 1000 mm (3.281 ft)

Channel width: 1000 mm (3.281 ft)

Crest height above channel bottom: 1133 mm (3.717 ft)

Run #	Head (mm)	Discharge (l/s)	Head (ft)	Discharge (cfs)
15-1	200	188	0.656	6.64
15-2	250	262	0.820	9.25
15-3	301	346	0.988	12.22
15-4	353	435	1.158	15.36
15-5	399	521	1.309	18.40
15-6	444	608	1.457	21.47

Gate angle: 45.00°

Weir width: 1000 mm (3.281 ft)

Channel width: 1000 mm (3.281 ft)

Crest height above channel bottom: 1133 mm (3.717 ft)

Run #	Head (mm)	Discharge (l/s)	Head (ft)	Discharge (cfs)
16-1	201	193	0.659	6.82
16-2	253	274	0.830	9.68
16-3	301	354	0.988	12.50
16-4	352	444	1.155	15.68
16-5	398	532	1.306	18.79
16-6	436	605	1.431	21.37

Gate angle: 45.00°

Weir width: 1000 mm (3.281 ft)

Channel width: 1000 mm (3.281 ft)

Crest height above channel bottom: 352.0 mm (1.155 ft)

Run #	Head (mm)	Discharge (l/s)	Head (ft)	Discharge (cfs)
28-1	201	196	0.659	6.92
28-2	302	371	0.991	13.10
28-3	391	559	1.283	19.74

Gate angle: 26.57°

Weir width: 1000 mm (3.281 ft)

Channel width: 1000 mm (3.281 ft)

Crest height above channel bottom: 1137 mm (3.730 ft)

Run #	Head (mm)	Discharge (l/s)	Head (ft)	Discharge (cfs)
17-1	205	203	0.673	7.17
17-2	302	361	0.991	12.75
17-3	401	551	1.316	19.46

Gate angle: 26.57°

Weir width: 1000 mm (3.281 ft)

Channel width: 1000 mm (3.281 ft)

Crest height above channel bottom: 351.1 mm (1.152 ft)

Run #	Head (mm)	Discharge (l/s)	Head (ft)	Discharge (cfs)
29-1	203	201	0.666	7.10
29-2	299	370	0.981	13.07
29-3	390	564	1.280	19.92

Gate angle: 14.04°

Weir width: 1000 mm (3.281 ft)

Channel width: 1000 mm (3.281 ft)

Crest height above channel bottom: 1133 mm (3.717 ft)

Run #	Head (mm)	Discharge (l/s)	Head (ft)	Discharge (cfs)
18-1	208	201	0.682	7.10
18-2	304	355	0.997	12.54
18-3	404	542	1.326	19.14

Gate angle: 14.04°

Weir width: 1000 mm (3.281 ft)

Channel width: 1000 mm (3.281 ft)

Crest height above channel bottom: 348.1 mm (1.142 ft)

Run #	Head (mm)	Discharge (l/s)	Head (ft)	Discharge (cfs)
30-1	202	192	0.663	6.78
30-2	299	359	0.981	12.68
30-3	404	577	1.326	20.38

**APPENDIX IX. DATA FOR USBR'S EXPERIMENTS ON INCLINED WEIRS**

Gate angle: 71.57°  
 Weir width: 614.8 mm (2.017 ft)  
 Channel width: 630.6 mm (2.069 ft)

Run #	Gate Height (mm)	Head (mm)	Discharge (l/s)	Head (ft)	Discharge (cfs)
13-3	1548.4	160.9	76.5	0.528	2.70
13-2	1548.4	178.6	89.1	0.586	3.15
13-1	1548.4	212.8	116.6	0.698	4.12
16-1	612.6	186.2	95.4	0.611	3.37
15-1	765.0	232.6	133.8	0.763	4.73
14-1	996.7	349.0	241.3	1.145	8.52
16-2	612.6	292.6	192.7	0.960	6.81
15-2	765.0	371.9	277.2	1.220	9.79
15-3	759.0	377.6	281.0	1.239	9.93
17-1	460.2	232.3	136.2	0.762	4.81
17-2	454.2	367.0	279.3	1.204	9.86
18-1	303.9	256.0	162.4	0.840	5.74
19-1	192.0	162.2	82.8	0.532	2.93
19-2	192.0	228.9	141.6	0.751	5.00
18-2	302.4	361.2	282.6	1.185	9.98
21-1	121.0	151.2	75.5	0.496	2.67
19-3	191.4	306.6	227.8	1.006	8.05
20-2	166.4	267.9	184.3	0.879	6.51
21-2	120.7	195.7	115.7	0.642	4.09
27-2	126.2	237.7	179.4	0.780	6.34
20-1	168.9	339.9	274.4	1.115	9.69
23-1	97.5	201.2	124.6	0.660	4.40
25-1	70.7	150.9	79.6	0.495	2.81
21-3	119.8	256.0	179.8	0.840	6.35
22-1	107.6	274.6	205.6	0.901	7.26
25-2	72.2	190.2	116.7	0.624	4.12
23-2	97.8	261.5	191.0	0.858	6.75
24-1	81.1	250.5	183.8	0.822	6.49
25-3	71.3	237.1	169.9	0.778	6.00
27-4	44.5	148.1	83.3	0.486	2.94
25-4	71.3	283.2	229.4	0.929	8.10
24-2	80.2	325.8	284.0	1.069	10.03
27-3	43.3	178.3	114.4	0.585	4.04
26-1	52.1	270.1	217.5	0.886	7.68
28-2	23.2	147.5	85.9	0.484	3.04
27-1	40.2	298.4	260.7	0.979	9.21
28-1	21.9	215.5	156.0	0.707	5.51
28-3	21.0	302.4	263.2	0.992	9.30

Gate angle: 56.31°  
 Weir width: 614.8 mm (2.017 ft)  
 Channel width: 630.6 mm (2.069 ft)

Run #	Gate Height (mm)	Head (mm)	Discharge (l/s)	Head (ft)	Discharge (cfs)
29-3	1439.0	159.4	77.3	0.523	2.73
29-2	1439.0	182.0	94.3	0.597	3.33
29-1	1439.9	217.6	124.9	0.714	4.41
32-1	460.6	214.9	124.7	0.705	4.41
31-1	611.7	287.1	191.1	0.942	6.75
30-1	756.5	360.0	269.3	1.181	9.51
34-1	193.5	217.9	135.5	0.715	4.79
36-1	123.4	139.3	69.5	0.457	2.46
33-1	269.7	308.5	226.7	1.012	8.01
37-1	100.0	192.0	118.4	0.630	4.18
35-1	145.1	284.4	212.1	0.933	7.49
36-2	123.7	244.1	170.2	0.801	6.01
38-1	84.7	254.2	192.6	0.834	6.80
40-1	72.5	222.8	158.6	0.731	5.60
42-1	46.0	150.3	86.4	0.493	3.05
39-1	72.8	267.6	215.5	0.878	7.61
41-1	53.3	204.2	143.0	0.670	5.05
42-2	46.0	177.4	114.4	0.582	4.04
41-2	53.0	237.4	184.5	0.779	6.52
43-1	38.7	176.8	117.5	0.580	4.15
44-1	26.2	145.1	85.1	0.476	3.01
43-2	39.0	228.0	177.1	0.748	6.26
44-2	25.6	190.8	133.2	0.626	4.71

Gate angle: 45.00°  
 Weir width: 614.8 mm (2.017 ft)  
 Channel width: 630.6 mm (2.069 ft)

Run #	Gate Height (mm)	Head (mm)	Discharge (l/s)	Head (ft)	Discharge (cfs)
45-3	1287.5	160.6	79.9	0.527	2.820
45-2	1286.9	167.3	84.7	0.549	2.990
45-1	1286.6	202.7	113.7	0.665	4.015
46-1	757.1	340.8	252.2	1.118	8.905
48-1	463.9	215.2	127.7	0.706	4.510
47-1	614.8	289.6	196.8	0.950	6.950
50-1	190.8	206.0	126.4	0.676	4.465
49-1	269.4	295.4	216.2	0.969	7.635
52-2	118.0	131.4	63.9	0.431	2.255
51-1	142.6	268.2	198.5	0.880	7.010
53-1	96.6	182.3	111.1	0.598	3.925
52-1	117.0	224.6	153.1	0.737	5.405
54-1	83.2	239.0	178.1	0.784	6.290
58-1	45.7	135.0	75.5	0.443	2.665
56-1	71.6	235.0	177.0	0.771	6.250
57-1	54.6	181.7	122.9	0.596	4.340
55-1	78.9	265.2	214.2	0.870	7.565
58-2	46.0	158.8	99.7	0.521	3.520
58-3	46.0	192.3	137.6	0.631	4.860
57-2	51.8	223.7	170.9	0.734	6.035
60-1	24.4	112.8	59.7	0.370	2.110
59-1	40.2	200.9	150.4	0.659	5.310
60-2	24.1	144.2	89.2	0.473	3.150

**APPENDIX X. DATA FROM FIELD EXPERIMENTS ON FREE-FLOW OVERSHOT GATES**

Location: Plum Canal, IID  
 Test date: August 18, 1993  
 Gate blade length: 1549 mm (5.083 ft)  
 Gate width: 1631 mm (5.35 ft)

Run #	Gate Angle (°)	Head (mm)	Discharge (l/s)	Head (ft)	Discharge (cfs)
1	47.3	134.4	169.9	0.441	6.00
2	41.9	178.9	263.9	0.587	9.32
3	40.3	181.4	266.4	0.595	9.41
4	39.1	174.7	246.3	0.573	8.70
5	37.5	164.3	232.3	0.539	8.20
6	37.0	170.1	240.2	0.558	8.48
7	33.2	186.5	259.4	0.612	9.16
8	28.8	186.8	274.9	0.613	9.71
9	25.3	186.2	262.2	0.611	9.26

Location: Oasis Canal, IID  
 Test date: November 16, 1993  
 Gate blade length: 1702 mm (5.583 ft)  
 Gate width: 1631 mm (5.35 ft)

Run #	Gate Angle (°)	Head (mm)	Discharge (l/s)	Head (ft)	Discharge (cfs)
1-1	33.4	391.7	828.9	1.285	29.27
1-2	31.0	392.6	861.8	1.288	30.43
1-3	28.2	390.4	861.8	1.281	30.43
1-4	26.6	388.9	859.4	1.276	30.35
1-5	21.2	385.9	863.0	1.266	30.48
1-6	19.8	384.0	872.9	1.260	30.83
1-7	16.8	370.9	880.3	1.217	31.09

Location: Oasis Canal, IID  
 Test date: November 16, 1993  
 Gate blade length: 1702 mm (5.583 ft)  
 Gate width: 1631 mm (5.35 ft)

Run #	Gate Angle (°)	Head (mm)	Discharge (l/s)	Head (ft)	Discharge (cfs)
2-1	35.8	351.7	747.8	1.154	26.41
2-2	32.6	353.9	746.6	1.161	26.37
2-3	28.0	353.0	747.8	1.158	26.41
2-4	26.2	349.9	747.8	1.148	26.41
2-5	23.8	349.9	745.5	1.148	26.33
2-6	21.2	348.1	747.8	1.142	26.41
2-7	19.2	342.3	746.6	1.123	26.37
2-8	17.2	332.8	748.9	1.092	26.45

Location: Oasis Canal, IID  
 Test date: November 17, 1993  
 Gate blade length: 1702 mm (5.583 ft)  
 Gate width: 1631 mm (5.35 ft)

Run #	Gate Angle (°)	Head (mm)	Discharge (l/s)	Head (ft)	Discharge (cfs)
3-1	42.8	305.4	601.9	1.002	21.25
3-2	39.6	309.4	602.9	1.015	21.29
3-3	37.2	304.5	608.1	0.999	21.47
3-4	34.6	305.7	607.0	1.003	21.44
3-5	32.4	305.4	606.0	1.002	21.40
3-6	29.0	304.5	602.9	0.999	21.29
3-7	26.8	306.3	605.0	1.005	21.36
3-8	24.4	302.4	602.9	0.992	21.29
3-9	22.2	301.4	601.9	0.989	21.25
3-10	20.2	300.2	601.9	0.985	21.25
3-11	18.2	296.0	602.9	0.971	21.29

Location: Oasis Canal, IID  
 Test date: November 17, 1993  
 Gate blade length: 1702 mm (5.583 ft)  
 Gate width: 1631 mm (5.35 ft)

Run #	Gate Angle (°)	Head (mm)	Discharge (l/s)	Head (ft)	Discharge (cfs)
4-1	43.8	264.3	486.2	0.867	17.17
4-2	40.6	260.6	484.3	0.855	17.10
4-3	37.4	261.5	487.1	0.858	17.20
4-4	36.2	259.4	483.4	0.851	17.07
4-5	32.4	259.7	485.3	0.852	17.14
4-6	29.8	256.9	486.2	0.843	17.17
4-7	28.2	258.8	480.6	0.849	16.97
4-8	24.6	257.6	483.4	0.845	17.07
4-9	20.6	258.5	482.5	0.848	17.04
4-10	16.9	252.4	483.4	0.828	17.07

Location: Oasis Canal, IID  
 Test date: November 18, 1993  
 Gate blade length: 1702 mm (5.583 ft)  
 Gate width: 1631 mm (5.35 ft)

Run #	Gate Angle (°)	Head (mm)	Discharge (l/s)	Head (ft)	Discharge (cfs)
5-1	49.0	218.2	351.8	0.716	12.42
5-2	44.4	215.8	358.2	0.708	12.65
5-3	40.2	213.7	357.4	0.701	12.62
5-4	35.4	214.9	359.0	0.705	12.68
5-5	31.8	219.8	358.2	0.721	12.65
5-6	28.0	219.8	357.4	0.721	12.62
5-7	26.2	215.2	358.2	0.706	12.65
5-8	24.0	214.9	359.0	0.705	12.68
5-9	22.2	211.8	355.0	0.695	12.54
5-10	20.2	212.4	358.2	0.697	12.65
5-11	18.2	209.1	358.2	0.686	12.65
5-12	15.0	196.3	356.6	0.644	12.59

Data points in italics indicate runs in which full ventilation of the leaf gate was not obtained.

# APPENDIX XI. DATA FROM FIELD EXPERIMENTS ON SUBMERGED OVERSHOT GATES

Location: Oasis Canal, IID

Test date: November 18, 1993

Gate angle: 22.2°

Free-overfall head: 211.8 mm (0.695 ft)

Discharge: 358.1 l/s (12.65 cfs)

Upstream Head (mm)	Downstream Head (mm)	Upstream Head (ft)	Downstream Head (ft)
216.1	31.1	0.709	0.102
219.5	40.5	0.720	0.133
219.2	46.3	0.719	0.152
221.3	55.2	0.726	0.181
223.1	63.7	0.732	0.209
223.7	73.8	0.734	0.242
228.3	101.8	0.749	0.334
237.4	142.0	0.779	0.466
242.6	159.7	0.796	0.524

